Where are we with calibration under dataset shift in image classification?

Mélanie Roschewitz *m.roschewitz21@imperial.ac.uk*
Imperial College London

Raghav Mehta *raghav.mehta@imperial.ac.uk*
Imperial College London

Fabio De Sousa Ribeiro *f.de-sousa-ribeiro@imperial.ac.uk*
Imperial College London

Ben Glocker *b.glocker@imperial.ac.uk*
Imperial College London

Reviewed on OpenReview: *https://openreview.net/forum?id=1NYKXlRU2H*

Abstract

We conduct an extensive study on the state of calibration under real-world dataset shift for image classification. Our work provides important insights on the choice of post-hoc and in-training calibration techniques, and yields practical guidelines for all practitioners interested in robust calibration under shift. We compare various post-hoc calibration methods, and their interactions with common in-training calibration strategies (e.g., label smoothing), across a wide range of natural shifts, on eight different classification tasks across several imaging domains[1]. We find that: (i) simultaneously applying entropy regularisation and label smoothing yield the best calibrated raw probabilities under dataset shift, (ii) post-hoc calibrators exposed to a small amount of semantic out-of-distribution data (unrelated to the task) are most robust under shift, (iii) recent calibration methods specifically aimed at increasing calibration under shifts do not necessarily offer significant improvements over simpler post-hoc calibration methods, (iv) improving calibration under shifts often comes at the cost of worsening in-distribution calibration. Importantly, these findings hold for randomly initialised classifiers, as well as for those finetuned from foundation models, the latter being consistently better calibrated compared to models trained from scratch. Finally, we conduct an in-depth analysis of ensembling effects, finding that (i) applying calibration prior to ensembling (instead of after) is more effective for calibration under shifts, (ii) for ensembles, OOD exposure deteriorates the ID-shifted calibration trade-off, (iii) ensembling remains one of the most effective methods to improve calibration robustness and, combined with finetuning from foundation models, yields best calibration results overall.

1 Introduction

Reliable uncertainty estimation is paramount to the development of trustworthy machine learning models. Models should accurately estimate their level of uncertainty, without being over- or under-confident in their predictions. Model calibration precisely measures how well predicted confidence scores reflect the likelihood of model predictions to be correct (Murphy, 2023; Guo et al., 2017). Calibrated probabilities are more interpretable and enable reliable performance estimation post-deployment. Improving calibration has been

[1]Our code is publicly available at https://github.com/biomedia-mira/calibration_under_shifts

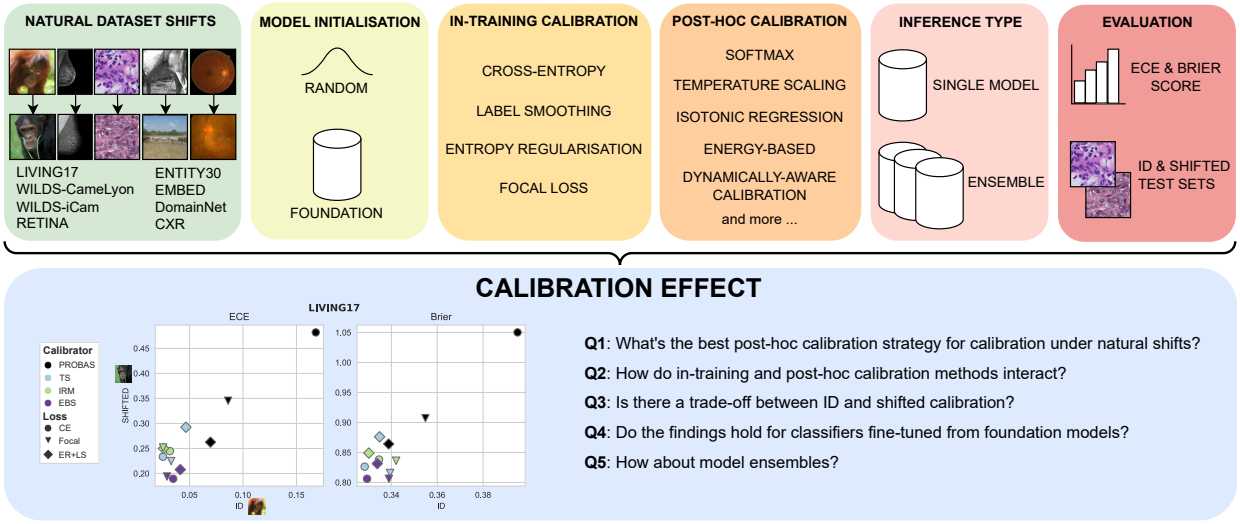

Figure 1: **Overview of our calibration study**.

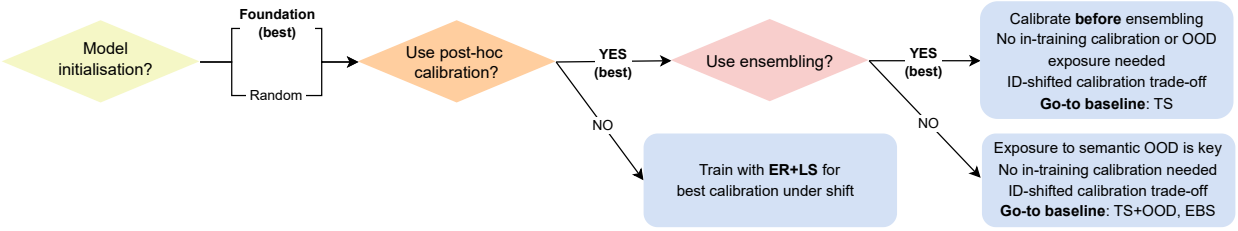

Figure 2: **Practical guidelines for improved calibration under dataset shifts**.

the topic of many papers over the last few years, across various tasks (Guo et al., 2017; Szegedy et al., 2016; Müller et al., 2019; Mukhoti et al., 2020; Zadrozny & Elkan, 2002; Gupta et al., 2021; Zhang et al., 2020; Tomani et al., 2023; 2021; Seligmann et al., 2023; Kim & Kwon, 2024).

Dataset shift is an eminent issue for model calibration (Ovadia et al., 2019). Yet, for long, most of the field has concentrated on evaluating new calibration methods in in-distribution (ID) settings, where calibration and test sets come from the same distribution (Guo et al., 2017; Zhang et al., 2020; Pereyra et al., 2017; Mukhoti et al., 2020; Meister et al., 2020). While calibration under shifts is still largely under-studied, recently, an increasing number of studies specifically focus on this issue (Tomani et al., 2021; 2023; Kim & Kwon, 2024; Yuksekgonul et al., 2023). However, most of those exclusively rely on limited synthetic corruption datasets for evaluation, i.e. CIFAR-C, ImageNet-C (Hendrycks & Dietterich, 2018; Krizhevsky, 2009; Deng et al., 2009). Unfortunately, it is known that observations made on synthetic distribution shifts may not always hold on more realistic shifts (Taori et al., 2020; Koh et al., 2021). Hence, this paper aims to better understand existing calibration methods and identify which specific factors contribute to improved calibration under *realistic* dataset shifts, across various imaging domains.

A large portion of the calibration literature has focused on developing post-hoc methods, allowing to correct model under/over-confidence after training. These, for example, include temperature scaling (Guo et al., 2017) or isotonic regression (Zadrozny & Elkan, 2002; Zhang et al., 2020). Others have instead proposed to address miscalibration directly during training, developing specific loss functions and training strategies (Mukhoti et al., 2020; Müller et al., 2019; Pereyra et al., 2017). Prominent examples include label smoothing, entropy regularisation, and focal loss, which are now widely used and part of the standard implementation of most deep learning frameworks. However, there is a need for a more in-depth look at their behaviour under natural dataset shifts. Moreover, some studies suggest that such in-training calibration methods may suffer from 'negative calibration' i.e., their calibration worsens when combined with posthoc

calibration methods (Wang et al., 2021; Zhang et al., 2022). This prompts us to not only study in-training and post-hoc calibration methods in isolation, but also to carefully examine their interaction across a wide range of shifts.

Meanwhile, foundation models have emerged as a promising avenue to improve model robustness (Oquab et al., 2023; Zhang et al., 2025; Zhou et al., 2023; Shi et al., 2024; Mehta et al., 2022). Hence, we also investigate the calibration of classifiers finetuned from these large foundation models. Specifically, we aim to understand whether: (i) the findings for randomly initialised classifiers generalise to classifiers finetuned from foundation models, (ii) calibration under dataset shifts is indeed improved compared to models trained from scratch.

Finally, perhaps the most common approach to increase robustness under shifts, when the computational budget allows, is ensembling (Lakshminarayanan et al., 2017). Many studies showed that ensembling can significantly help with model robustness and calibration (Seligmann et al., 2023; Kumar et al., 2022). However, there is also some contradictory evidence suggesting that deep ensembles are not necessarily better calibrated than individual ensemble members (Rahaman & Thiery, 2021; Kumar et al., 2022). Hence, we conclude our study by analysing ensemble calibration, comparing the effect of various calibration methods, and in particular, the impact of applying calibration before or after ensembling.

To summarise, as illustrated in Fig. 1, we comprehensively study existing in-training and post-hoc calibration methods, specifically investigating their impact on calibration under dataset shifts. *Our goal is not to propose a new method, but rather to find practical guidelines on which methods to choose for obtaining well-calibrated probability under shifts.* Our study covers eight datasets and tasks, a wide range of imaging modalities from satellite images to mammography and histopathology images. We focus on realistic distribution shifts, from geographical location shifts, medical device shifts, sub-population shifts, experimental protocols shifts, and more. We study the effect of five different in-training calibration methods and their interactions with ten post-hoc calibration methods. We evaluate models trained from random initialisation as well as finetuned from foundation models, across various CNN- and transformer-based architectures, training 420 models in total. Finally, we analyse the effect of model ensembling on calibration under shifts, compare various ensemble calibration strategies and study interactions between ensemble calibration and calibration of individual ensemble members.

The breadth of our analysis enables us to derive clear practical guidelines for practitioners interested in building classification systems with robust calibration under real-world shift, which we summarise in Fig. 2 and detail below, we find that:

(i) Classifiers fine-tuned from foundation models offer significantly better calibration (shifted and ID) compared to classifiers trained from scratch, regardless of the calibration strategy (§4.2.2);

(ii) In-training calibration is not needed when post-hoc calibration is used (§4.1.2);

(iii) Ensembling improves both ID and shifted calibration regardless of the calibration strategy (§4.3.1);

(iv) Without ensembling, the most effective strategy to improve calibration under shifts consists of adding small amounts of OOD data (unrelated to the task) to the calibration set, regardless of the choice of post-hoc calibrator (§4.1.1);

(v) For model ensembles, the best strategy to obtain robust calibration under shifts consists of applying post-hoc calibration *prior* to ensembling, and *without* OOD exposure (§4.3.2);

(vi) Improving calibration under shifts often comes at the cost of ID calibration (§4.1.3, §4.3.3).

We make all of our code available to the research community to facilitate further developments in this space.

2 Related work

Model calibration has been a prolific area of research. Proposed approaches notably include post-hoc calibration methods (Guo et al., 2017; Kim & Kwon, 2024; Zhang et al., 2020), alterations to loss functions (Szegedy

et al., 2016; Pereyra et al., 2017; Mukhoti et al., 2020), model ensembling (Lakshminarayanan et al., 2017) and Bayesian Neural Networks (BNN) (Detommaso et al., 2022; Maddox et al., 2019). In this study, we focus on popular calibration methods, which can be applied within standard training pipelines and for any model architecture. In particular, we consider the comparison of various BNN training strategies for calibration robustness out-of-scope. However, the reader interested in such a comparison is invited to consult Seligmann et al. (2023).

2.1 Model calibration metrics

We consider a classification task with C classes. Let $\hat{\mathbf{p}} \in [0,1]^C$ denote the model predicted probabilities with $\arg\max_i \hat{p}_i$ the predicted class and y the associated label. A model is said to be well calibrated if the probability associated with the predicted class (a.k.a. confidence score) matches the true probability of being correctly classified (Guo et al., 2017). Several metrics have been proposed to evaluate the calibration of a given model. The most popular one is the Expected Calibration Error or ECE (Guo et al., 2017), approximating the expected difference between predicted confidence and prediction accuracy (see Appendix A.2). Despite its popularity, a major limitation of ECE (and its variants like AdaECE, SCE (Nixon et al., 2019)) resides in the necessity of introducing a binning scheme, which may influence the calibration measure and make the metric sensitive to small test set sizes (Nixon et al., 2019; Gruber & Buettner, 2022). An alternative metric is, for example, the Brier Score (Brier, 1950), which does not require any binning, is a proper score, and measures total calibration (as opposed to only top-level calibration like ECE). This score computes the average mean squared error between probabilities and one-hot labels (details in Appendix A.2).

2.2 In-training model calibration techniques

Several works have proposed specific loss functions and regularisation schemes tailored to improve the calibration of model outputs during training, without requiring any architectural changes. These include: label smoothing (LS) (Szegedy et al., 2016; Müller et al., 2019), entropy regularisation (ER) (Pereyra et al., 2017; Meister et al., 2020), and focal loss (Mukhoti et al., 2020). In LS, labels are softened to explicitly discourage the network from being too confident in its predictions, i.e. $\tilde{\mathbf{y}} = (1-\lambda)\mathbf{y} + \lambda\frac{1}{C}$, with $\mathbf{y}$ the one-hot encoded labels, and λ the hyperparameter controlling the amount of smoothing (typically ranging in $[0.01, 0.1]$). ER adds the negative entropy of the predictions to the cross-entropy loss, where the strength of the regularisation is controlled by a multiplicative constant α (with $\alpha = 0.1$ working well across tasks (Pereyra et al., 2017)). Another popular approach is the focal loss (Lin et al., 2020), defined as $\sum_{k=1}^{C} y_k(1-\hat{p}_k)^\gamma \log(\hat{p}_k)$, where γ is an hyperparameter. Mukhoti et al. (2020) show that focal loss can improve model calibration, in particular when using $\gamma = 5$ if $\hat{p}_k \in [0, 0.2)$ else $\gamma = 3$. Note that other variants of these losses have been subsequently proposed (Meister et al., 2020; Liu et al., 2022); however, here, we focus on LS, ER, and focal losses as these remain the most popular for image classification (Gao et al., 2020; Wei et al., 2022; Wang et al., 2022; Carse et al., 2022; Fuentes et al., 2023).

2.3 Post-hoc model calibration techniques

Modifying the loss function to improve calibration is not always a practical solution, as one may not always have full control over the training process, and loss function alterations may have inadvertent side effects, such as performance reduction. Hence, many have focused on developing *post-hoc* recalibration techniques to address mis-calibration after training. This paradigm has the advantage of being independent of the model architecture or the choice of the loss function during training and is widely used in practice. One example of such post-hoc calibration method is temperature scaling (TS) (Guo et al., 2017) (or Platt-scaling), where the logits $\mathbf{z}$ are scaled by a constant T, where T is tuned on the validation set such that the negative likelihood is minimised. Calibrated probabilities are then obtained with $\hat{\mathbf{p}} = \text{softmax}(\mathbf{z}/T)$. Adjusting the temperature controls the 'peakiness' of the distribution, allowing to correct for model over/under-confidence. Another approach consists of using isotonic regression (IRM) (Zadrozny & Elkan, 2002) between the predicted probabilities and the expected accuracy (non-parametric). Gupta et al. (2021) have alternatively proposed to use splines for calibrating outputs (SPL). The synergies between various parametric and non-parametric post-hoc methods have been explored by Zhang et al. (2020), who notably proposed ETS, an ensemble formulation

of TS to allow for increased expressivity. They also proposed IROVaTS, combining IROVa (IRM in a one-versus-all setup for a multiclass problem) with ETS. Recently, Kim & Kwon (2024) proposed energy-based calibration (EBS), utilising the energy of the logits, i.e., $\mathcal{F}(\mathbf{z}) = -\text{logsumexp}(\mathbf{z})$ to derive a sample-wise temperature. Importantly, this method utilises both an ID validation set and an out-of-distribution (OOD) set, semantically unrelated to the task, to improve calibration on shifted data (contrary to previous methods, which do not explicitly require access to external OOD data for calibration). More details on EBS can be found in Appendix A.5.1. Importantly, TS, ETS, IRM, and EBS are all accuracy-preserving, i.e., the final class prediction is unchanged after model calibration.

2.4 Calibration and the problem of dataset shift

An increasing number of studies have recently focused on increasing the robustness of model calibration under dataset shift. An early study from Tomani et al. (2021) proposed to apply random augmentations to images in the validation set used to fit post-calibrators, for better results under shifts. However, the generalisation of such calibrators is bounded by the ability of these random augmentations to faithfully capture shifts encountered at test-time. Yu et al. (2022) have, on the other hand, proposed to train a domain-to-temperature regressor. However, this requires access to multiple domains at validation time and for them to capture test-time shifts reliably – a highly impractical assumption. Instead Tomani et al. (2023) proposed Density-Aware-Calibration (DAC), leveraging nearest neighbours distances in the embedding space (at different layers throughout the network) to modulate the temperature for each sample, without requiring access to multiple domains at calibration time; this idea of measuring the sample's 'atypicality' to calibrate the network is also adopted in concurrent work from (Yuksekgonul et al., 2023). Importantly, DAC is a plug-in method that can be used in conjunction with any other post-hoc calibration method. Finally, Kim & Kwon (2024) demonstrated state-of-the-art results with their EBS calibrator against a wide range of post-hoc calibrators on CIFAR10-C and ImageNet-C (Hendrycks & Dietterich, 2018), with best results obtained when EBS is used in conjunction with DAC. Yet, more analyses are needed to determine the robustness of these calibration methods on a broader set of tasks and, crucially, on real-world shifts beyond synthetic image corruptions.

For the convenience of the reader, a comparative overview of prior work on calibration under shifts in image classification and our study is presented in Table A.2.

2.5 Model ensembling and calibration

Another popular approach to improve calibration is model ensembling (Lakshminarayanan et al., 2017). Kumar et al. (2022) showed that ensembling diverse calibrated models yields more robust models and better calibration across various tasks. Similarly, a recent study from Seligmann et al. (2023) on the calibration of Bayesian neural networks showed that ensembling was more efficient than any single Bayesian calibration method in terms of robustness under shifts. However, others report contradictory evidence as well. Wu & Gales (2021) provided theoretical insights on why calibration of individual ensemble members is not sufficient for their aggregate predictions to be well calibrated, and Rahaman & Thiery (2021) showed that deep ensembles are not necessarily better calibrated than individual ensemble members. These contradictory findings prompt us to include ensembling effects in our study.

3 Experimental setup

3.1 Datasets and studied shifts

We analyse calibration robustness across different image classification tasks and real-world natural distribution shifts. First, we investigate robustness against geographic and sub-population shifts, in natural image classification using the **Living17** and **Entity30** datasets (Santurkar et al., 2020), as well as **Wilds-iCam** (Koh et al., 2021). Next, we analyse realistic shifts specific to medical imaging, a high-stakes domain where robustness and calibration are of particular importance. We study calibration robustness against: (i) scanner changes in breast density assessment models using the **EMBED** (Jeong et al., 2023) mammography dataset, (ii) scanner, population and prevalence changes in chest X-ray classification (No Finding /

Dataset	Type of shift(s)	Task	N classes
Living17	Population	Balanced	17
Entity30	Population	Balanced	30
CameLyon	Staining	Balanced	2
CXR	Scanner, Prevalence, Population	Imbalanced	2
RETINA	Scanner, Prevalence, Population	Imbalanced	5
EMBED	Scanner	Imbalanced	4
iCam	Geographic, Prevalence	Imbalanced	182
DomainNet	Image type, Prevalence	Imbalanced	345

Table 1: Datasets and shifts used in this study.

Diseased) using CheXpert (Irvin et al., 2019) and MIMIC-CXR (Johnson et al., 2019) (**CXR**), (iii) equipment, prevalence, and geographic location changes for diabetic retinopathy assessment models, combining multiple public fundus imaging datasets (Karthik & Sohier, 2019; Decencière et al., 2014; Dugas et al., 2015) (**RETINA**), and (iv) staining protocols changes in histopathology, using **WILDS-CameLyon** (Koh et al., 2021). Finally, we test against hard modality shifts in natural image classification using **DomainNet** (Peng et al., 2019) with 'Real' images as the ID domain. Details about datasets and ID/shifted domain definitions can be found in Appendix A.1, including visual examples of samples from both ID and shifted test sets for each dataset.

3.2 Models

Experiments are performed in two settings. First, for models trained with randomly initialised weights, where for each dataset, we trained classifiers with six different architectures: ResNet18/50 (He et al., 2016), EfficientNet (Tan & Le, 2019), MobileNet (Howard et al., 2017), ViT-Base (Dosovitskiy et al., 2020), ConvNext-tiny (Liu et al., 2022), keeping the checkpoint with the highest balanced accuracy on the validation set. We additionally investigate the calibration of models finetuned from pretrained foundation models, using the vision encoders from Dino-V2-Base (Oquab et al., 2023), CLIP (Radford et al., 2021), SiG-LIP (Zhai et al., 2023), MAE-Base (He et al., 2021) and, for medical datasets only, BioMedClip (Zhang et al., 2025). Additional details regarding our training setup and hyperparameters can be found in Appendix A.4. All detailed training configurations are also available in our codebase to ensure reproducibility.

3.3 Benchmarked methods

In this study, we aim to analyse the robustness of existing post-hoc calibration methods and their interactions with in-training calibration strategies, on a large variety of shifts and tasks. In terms of post-hoc methods, we compare **TS** (Guo et al., 2017), **IROVaTS** (Zhang et al., 2020), **IRM** (Zadrozny & Elkan, 2002), and **EBS** (Kim & Kwon, 2024). EBS has been shown to achieve state-of-the-art performance on calibration under synthetic corruptions for CIFAR and ImageNet (Kim & Kwon, 2024). However, one crucial difference separates EBS from other calibrators: it requires exposure to a small 'semantic OOD' set for calibration. This set is *unrelated* to the classification task and independent of the tested modality/imaging domain. Following Kim & Kwon (2024), we use samples from the Textures (Cimpoi et al., 2014) dataset for this purpose. However, we consider that comparing 'standard' post-hoc calibrators, such as TS, IRM, etc., with EBS is 'unfair' since EBS gets some outlier exposure in the calibration step, and, by default, the others don't. Hence, to better understand whether any potential calibration gains from EBS should be attributed to the energy-based calibration approach or the use of semantic OOD data, we also compare with augmented versions of these standard post-hoc calibrators where the same semantic OOD set is used along with the ID calibration set in the calibration stage. This yields additional calibrators **TS + OOD**, **IRM + OOD**, **IROVaTS + OOD** (see Appendix A.5.2 for implementation details). Conversely, we also report results of energy-based calibration in the absence of semantic OOD exposure, referred to as **EBS-**. Finally, we investigate the impact of **DAC** (Tomani et al., 2021), designed to improve calibration under shift, in combination with various calibrators.

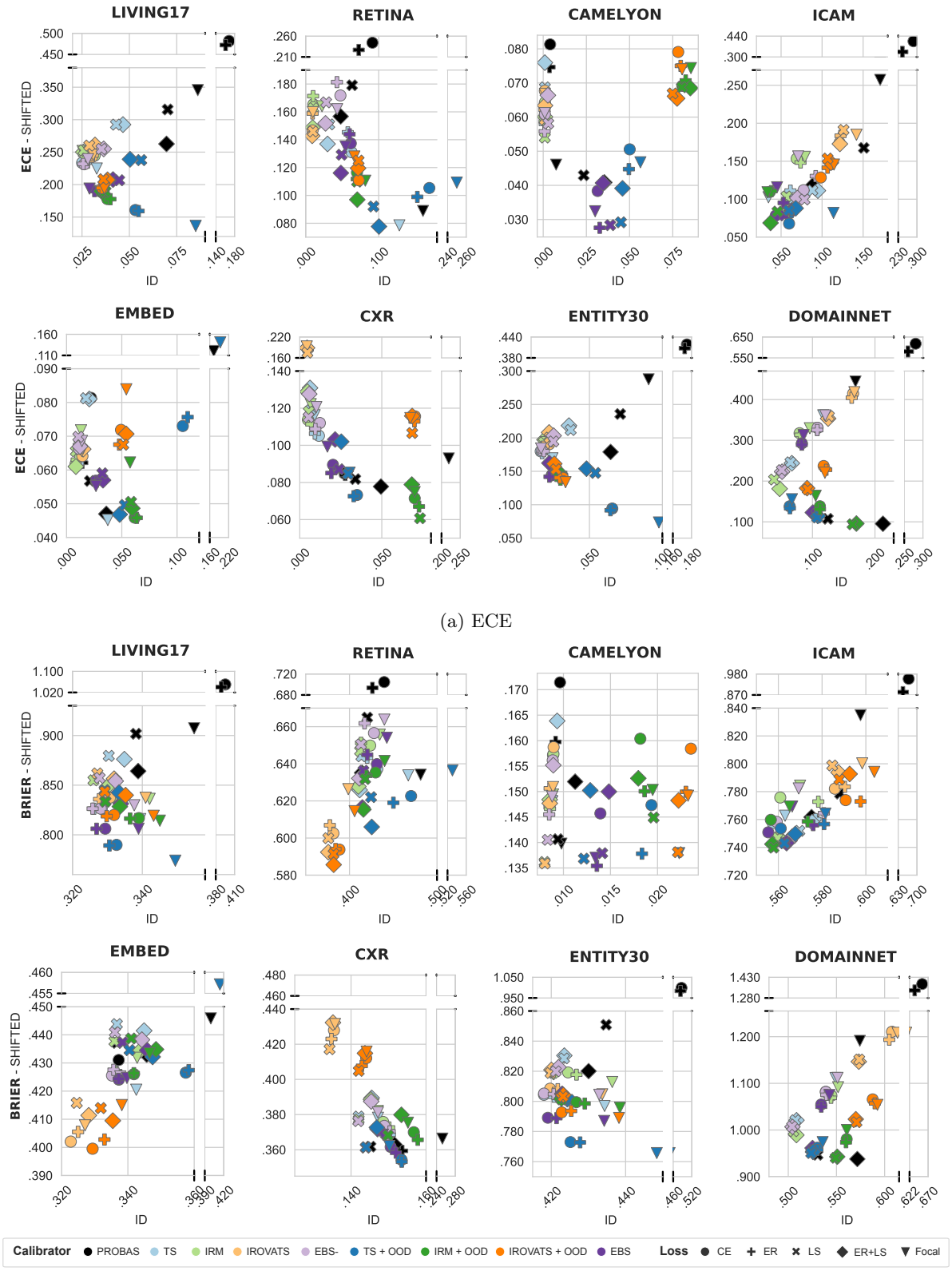

(a) ECE

(b) Brier Score

Figure 3: **Calibration under shifts in function of in-distribution calibration for classifiers with random weight initialisation:** For each dataset, we report average ECE (top) and Brier score (bottom), averaged over different models (6 architectures).

In terms of training strategies, we compare standard expected risk minimisation training with cross-entropy loss (**CE**), label smoothing (**LS**), entropy regularisation (**ER**), and **focal** loss. Moreover, given the symmetric effects of label smoothing and entropy regularisation, we also compare with a training strategy using both label smoothing and entropy regularisation simultaneously (**ER+LS**). We then analyse interactions between training strategies and post-hoc calibration methods. In terms of regularisation strength, we chose to fix the hyperparameters for the strength of label smoothing and entropy regularisation across all datasets and experiments ($\lambda = 0.05$ for LS, $\alpha = 0.1$ for ER, $\lambda = 0.05, \alpha = 0.1$ for ER+LS). Fixing these hyperparameters was a deliberate choice (chosen based on the best average ID calibration results across all datasets) to assess the generalisability of a given training strategy to new scenarios. Indeed, as we don't have access to the shifted test set in advance, we would not be able to tune those precisely for improving shifted calibration.

4 Results

We evaluate calibration using Expected Calibration Error (ECE) as well as the Brier Score. Whereas ECE focuses on top-label calibration, the Brier score measures full calibration and has the advantage of also taking model performance into account, offering two complementary measures of model calibration (see Section 2.1). In Fig. 3 (resp. Fig. 6), we report both ID and shifted calibration results for every combination of training loss and post-hoc calibration methods, for every dataset, for models trained from scratch (resp. finetuned from foundation models). In the following, we summarise the main take-aways from these experiments.

4.1 Calibration under shifts for models trained from scratch

4.1.1 Post-hoc calibration: exposure to semantic OOD significantly improves calibration under shift.

In Fig. 3, calibrators without semantic OOD exposure appear in lighter colours whereas their counterparts with exposure appear in darker colours. First, we notice that *after* post-hoc calibration, there is no consistent difference across the various tested training losses – no calibration-specific training loss consistently beats the standard cross-entropy loss. Most strikingly, across all datasets, we observe that calibrators with OOD exposure offer the best results in terms of calibration under shifts (y-axis), for both ECE and Brier scores, regardless of the training loss used. We, for example, find that surprisingly, simple temperature scaling with semantic exposure (TS + OOD) performs the most consistently across datasets and is at least as good as EBS, which was specifically designed for tackling calibration under shifts. Note that this improvement in calibration occurs even though the OOD data used is entirely unrelated to the task, and fixed across all evaluated datasets (Textures dataset, see Section 3.3). This shows that semantic OOD data does not need to be close to the ID images to benefit calibration. Some datasets, like Living17, are closer to images in the Textures dataset (RGB photos) while medical image datasets are further. In Fig. A.3, we confirm this by analysing differences between samples from the ID test set, from the shifted test sets and from the semantic OOD Textures in the embedding space across all datasets, showing that for some datasets the semantic OOD samples are much closer to the ID/shifted test sets than for others. However, results in Fig. 3 show that, regardless of the distance of the semantic OOD set to the ID data, adding exposure to these OOD images benefits calibration under shifts.

After statistical analysis, we confirm that calibrators with semantic OOD exposure have a significantly different effect over those without OOD exposure, however there are no significant differences across calibrators once controlling for semantic OOD exposure (see Appendix A.7 for details on statistical analysis). Regarding model performance, it is important to highlight that most post-hoc calibrators tested here are accuracy-preserving (TS, IRM, EBS), i.e. they do not affect the class prediction. Only IROVaTS affects model predictions and we note that it tends to worsen balanced accuracy both ID and under shifts, across datasets (see Fig. A.4).

Regarding the amount of semantic data to use for calibration, authors of EBS used pre-defined numbers of OOD images for their experiments on CIFAR/ImageNet, but no rationale was given on how to choose this number on new datasets. We found that the number of OOD samples has to be dependent on the size of the ID calibration set. In Fig. 4, we provide a detailed investigation of the sensitivity of various calibrators to the relative size of the OOD set. Results show that the ideal OOD size depends on the dataset, nevertheless,

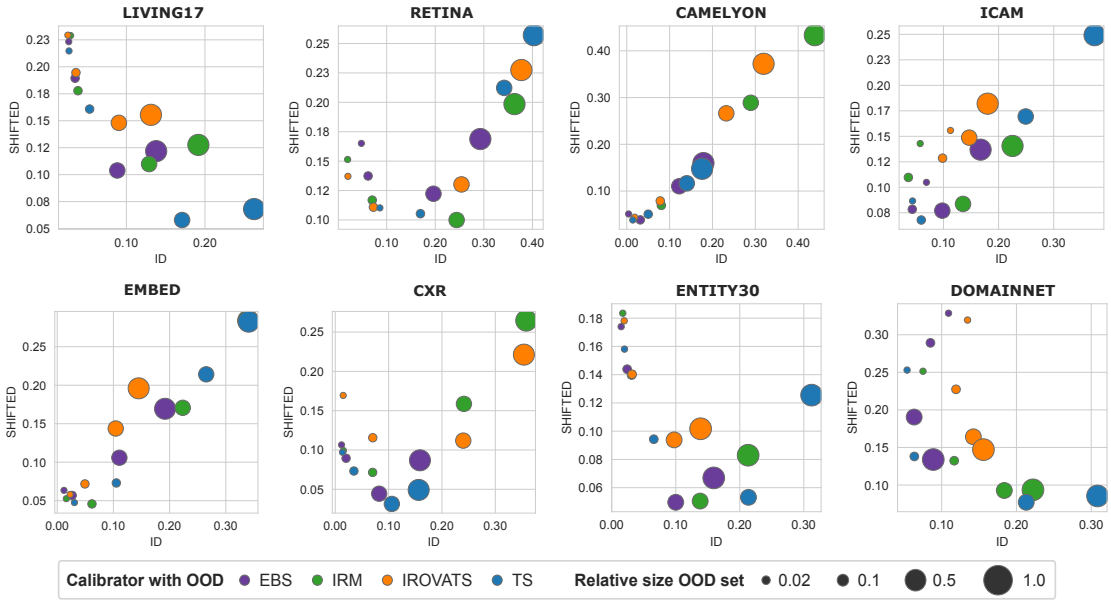

Figure 4: **Effect of the amount of semantic OOD data used for calibration on ECE:** (averaged over six model architectures). The amount of OOD data is here relative to the number of ID validation samples used to calibrate the model (varying across datasets).

we find that when the semantic OOD set is about 10% the size of ID validation set (used for calibration), the calibration performance lies on the Pareto front of ID-shifted calibration for most post-hoc calibrators and datasets. We chose this parametrisation across all experiments.

Finally, we additionally evaluate the effect of complementing post-hoc calibrators with Dynamically Aware Calibration (DAC). DAC uses distances in the embedding spaces to further optimise the sample-wise temperature and is compatible with many calibrators. Results in Fig. 5 suggest that DAC has mixed effects on model calibration, with substantial gains for some datasets (EMBED) and worsening calibration under shifts for others (IROVaTS/EBS CameLyon). Overall, it simply has little effect on many datasets (Living17, CXR, Entity30).

4.1.2 ER+LS training yields the best calibrated raw outputs on shifted data and is hard to beat with post-calibrators.

Without post-hoc calibration (black markers), models trained with both entropy-regularisation and label smoothing (ER+LS, diamond) are best calibrated, often by a large margin, both in terms of ECE and Brier score. For example, on Living17 and Entity30 the ECE is 50% lower for models trained with ER+LS than with CE. Overall, without post-hoc calibration, ER+LS has the lowest ECE across all tested training paradigms on 7 out of the 8 tested datasets, and the lowest Brier in 6 out of 8. Importantly, nor LS nor ER alone is able to reach the same consistent calibration robustness, combining both paradigms is key. Importantly, we find that the different loss functions perform similarly in terms of balanced accuracy across datasets (see Fig. A.4).

4.1.3 Improving calibration under shift often comes at the cost of ID calibration.

In Fig. 3, we observe that on several datasets (Living17, RETINA, CameLyon, CXR, Entity30) a trade-off pattern between ID and shifted calibration appears, in particular for ECE. This is particularly striking for calibrators with OOD exposure, which yield much lower calibration errors under shifts compared to other calibrators, but sometimes display substantially higher calibration error on ID test sets.

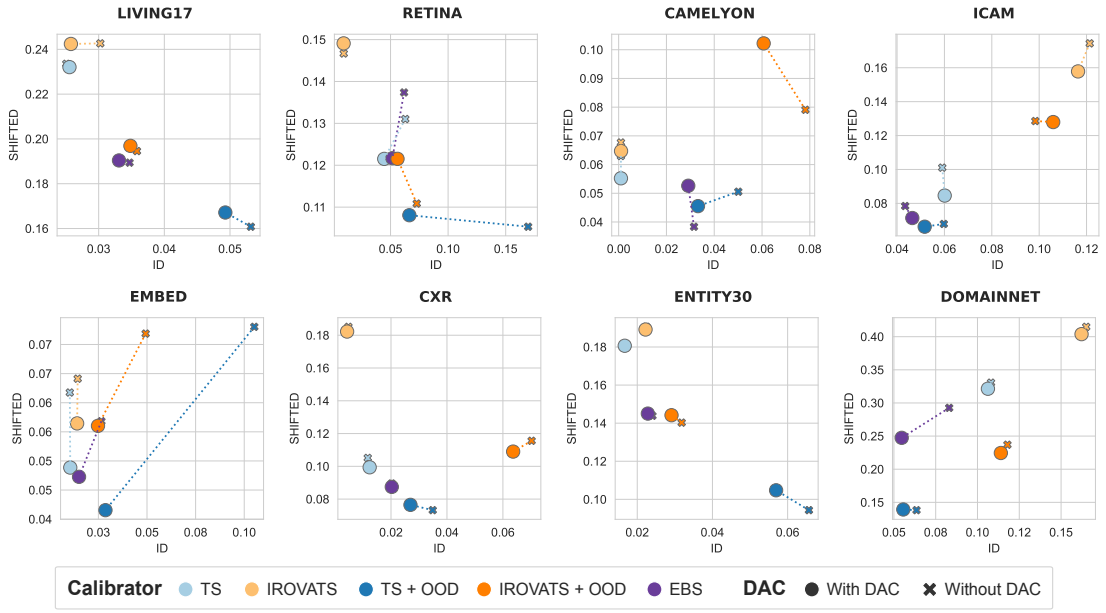

Figure 5: **Effect of DAC with various post-hoc calibrators on ECE: mixed results across datasets**. Large circles show calibration with DAC; crosses denote calibration without DAC. Full comparison with Brier score can be found in Appendix A.8.

4.2 Do these findings hold for classifiers finetuned from foundation models?

4.2.1 Findings from randomly initialised models generalise to models finetuned from foundation models

Fig. 6 compares calibration results both under shifts and on ID test sets, for classifiers finetuned from foundation models (averaged over four to five models, see Section 3.2). These results confirm our previous conclusions: exposure to semantic OOD improves calibration under shift, with EBS and TS+OOD yielding most consistent results in terms of ID-shifted trade-off across datasets (average ID-shifted calibration is best for TS+OOD on 6 out of 8 datasets). In terms of base predictions (without post-hoc calibration), models finetuned with ER+LS are best calibrated under shifts compared to base predictions from models trained with other losses (black markers, y-axis) on 6 out of 8 datasets, however this again often comes at the cost of ID calibration (3 out 6 datasets).

4.2.2 Models finetuned from foundation models are better calibrated under dataset shifts, irrespective of the calibrator used

In Fig. 6, the red star depicts average calibration for models trained from scratch (with CE) and using robust EBS post-hoc calibration, a strong baseline from Fig. 3. This comparison shows that models finetuned from foundation models offer substantially better calibration under dataset shifts, in terms of Brier score in particular (also reflecting an improvement in classification performance, see Fig. A.5), but also in terms of ECE. This conclusion may perhaps not be very surprising per se, however, it is important to note that even with foundation models applying robust post-hoc calibration like EBS or TS with semantic OOD significantly improves calibration compared to base probabilities. Moreover, a further ablation study in Fig. A.8 on the impact of model size on shifted-ID calibration demonstrates the calibration improvements are indeed attributable to the pretraining of the foundation models and not to their increased model size.

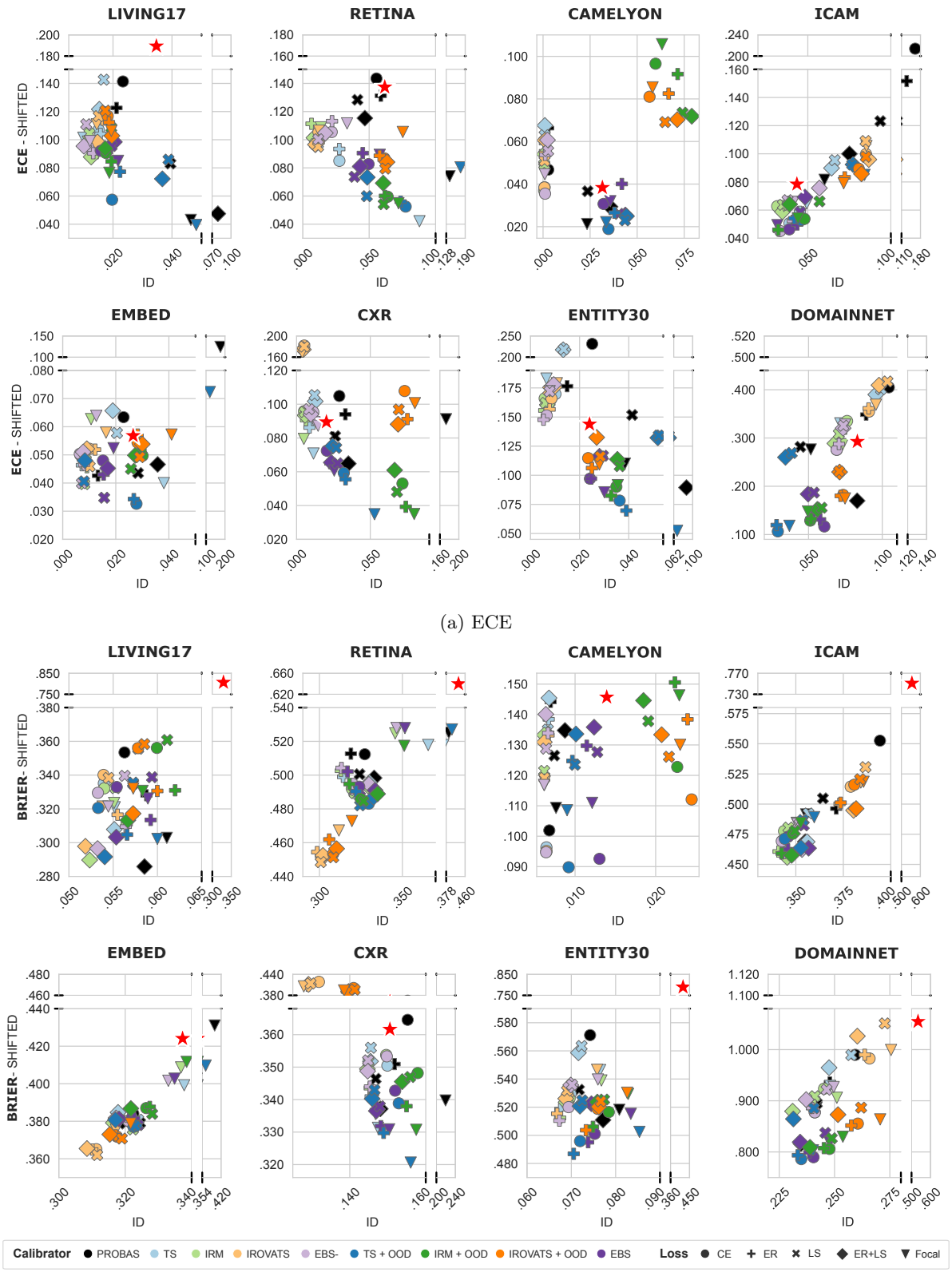

(a) ECE

(b) Brier score

Figure 6: **Calibration results for classifiers finetuned from foundation models:** top row ECE, bottom row Brier Score (average calibration finetuning four different foundation models, five for medical datasets). As a baseline, for each dataset, the red star depicts the average calibration of models trained from scratch with CE loss and EBS calibration.

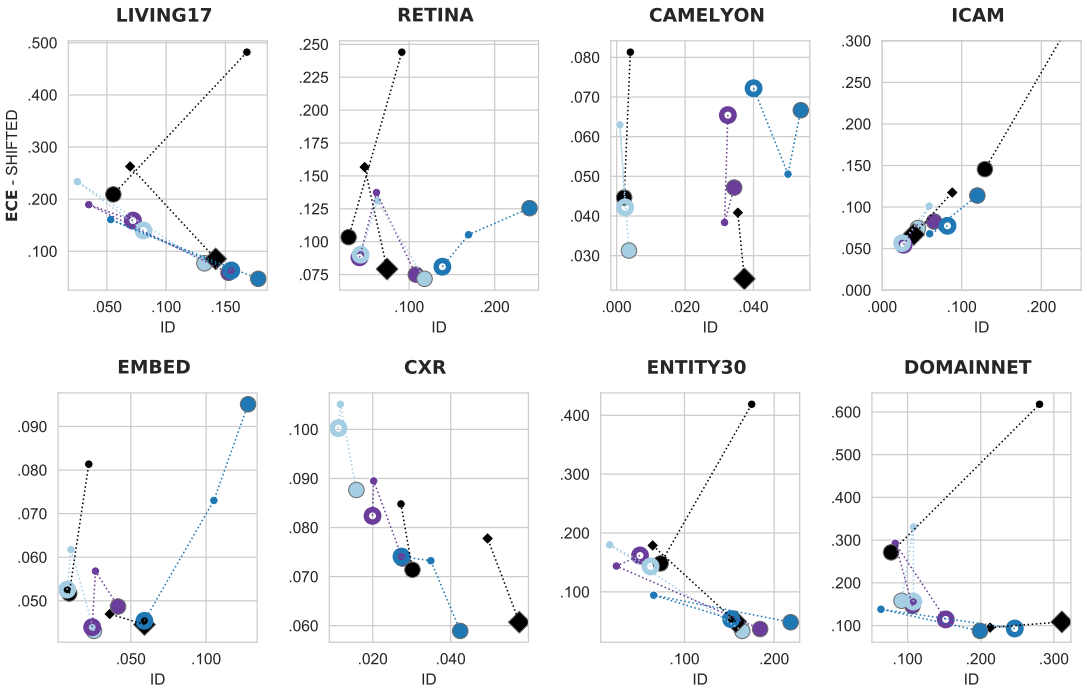

(a) Ensembles of classifiers trained from scratch.

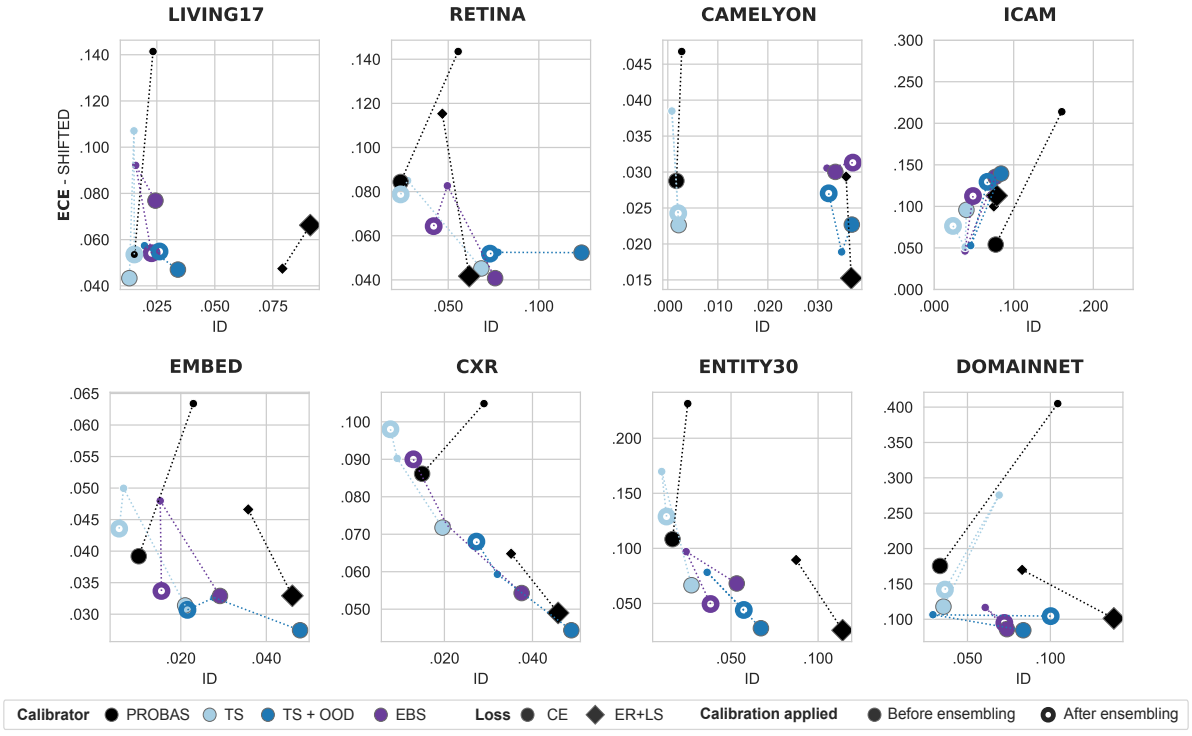

(b) Ensembles of classifiers finetuned from foundation models.

Figure 7: **Calibration of model ensembles in terms of ECE, in function of post-hoc calibration method**. Large dots denote calibration results for model ensembles, small dots the average calibration of individual ensemble members for reference. We compare the effect of (i) applying post-hoc calibration to ensemble members (before ensembling), (ii) applying post-hoc calibration after ensembling predictions.

4.3 Ensembles and shifted calibration

In light of conflicting results on the effect of model ensembling on calibration in the literature (see Section 2.5), we here investigate whether the previous findings experimentally generalise to model ensembles. For each dataset, we create various model ensembles by sampling random combinations of three models from the pool of previously trained classifiers. We investigate two types of ensembles: ensembles of classifiers trained from random initialisation and ensembles of classifiers finetuned from foundation models. In Fig. 7, we compare calibration results for different post-hoc calibrators when calibration is applied: (i) to individual ensemble members before ensembling or (ii) after ensembling (as argued in (Rahaman & Thiery, 2021)). Motivated by take-away 2, we additionally compare with ensembles of models trained with ER+LS.

4.3.1 Ensembling remains a very effective method for calibration

Fig. 7 shows that ensembles achieve better calibration under shifts compared to individual models (small versus large dots), irrespective of the calibration strategy. This is visible both in ECE and even more strikingly in the Brier score (also reflecting, as expected (Lakshminarayanan et al., 2017), an improvement in model performance after ensembling). Then, comparing results in Figs. 7a and 7b, we notice that calibration results lie in drastically different scales for ensembles of classifiers trained from scratch and ensembles of classifiers finetuned from foundation models. The latter being much better calibrated overall. Finally, in Figs. A.12 to A.15, we investigate whether these calibration gains depend on the size of the ensemble n, by comparing $n \in \{2, 3, 5\}$. We observe that calibration gains are already visible with ensembles with two members only. Gains on shifted calibration increase slightly as the number of members increases, however there is a plateau-effect with only minimal improvements when increasing from 3 to 5 ensemble members.

4.3.2 Applying post-hoc calibration *before* ensembling yields best calibration under shifts.

Comparing post-hoc calibration pre- and post-ensembling, results in Fig. 7 show that there is a clear trade-off between ID and shifted calibration in terms of ECE: doing TS (or EBS) after ensembling leads to better ID calibration, whereas TS (or EBS) before ensembling leads to better calibration on shifted datasets, and better overall ID-shifted calibration trade-off. For example, TS before ensembling (filled circles) systematically reaches a lower calibration error on shifted test sets compared to TS after ensembling (hollow circles). However, we observe the inverse pattern for ID test sets on Living17, Density, Retina, CXR, and Entity30. This finding also holds for models trained with ER+LS (see Fig. A.11). Finally, our ablation study on ensemble size in Figs. A.12 to A.15 shows that these conclusions hold for all ensemble sizes tested ($n = 2, 3, 5$).

Comparing TS and TS + OOD in Fig. 7 we find that semantic OOD exposure in post-hoc calibration often degrades calibration for shifted tests (y-axis, RETINA, EMBED, CameLyon) and even more so for ID test sets (x-axis). Interestingly, this is contrary to previous findings and independent of whether calibration is applied before or after ensembling. Further ablation studies in Fig. A.10 confirm this finding on additional post-hoc calibrators. These results suggest that, if the goal is to ensemble models, individual ensemble members should be calibrated with standard calibration methods, not with OOD exposure.

4.3.3 Without post-hoc calibration, ensembles whose members were trained with ER+LS are substantially better calibrated under shifts.

Finally, comparing ensemble calibration without post-hoc calibration (black markers in Fig. 7), we can, again, see that ensembles whose members were trained with ER+LS offer substantially better calibration results under shifts compared to ensembles whose members were trained with CE, across all datasets, for both ECE and Brier score. However, this often comes at the cost of worse ECE on ID test sets (Living17, Entity30, EMBED, CXR, DomainNet).

5 Conclusion

We conduct a large-scale experimental evaluation of calibration methods in the presence of realistic dataset shifts. Associated findings provide practical guidelines for constructing models with robust calibration under such shifts. First, for single models (i.e. without ensembling), we find that post-hoc calibrators exposed to task-agnostic OOD data performed best for calibration under shifts, particularly EBS and TS+OOD. This finding holds irrespective of the training paradigm, across datasets, for classifiers trained from scratch and finetuned from foundation models. Yet, this can come at the cost of worsening ID calibration, yielding an ID-shifted calibration trade-off. Moreover, and perhaps surprisingly, this finding does not hold for model ensembles, where we find that OOD exposure should *not* be used for calibration. Moreover, we find that models trained with entropy regularisation and label smoothing provided the best calibrated base probabilities for shifted test sets (without any post-hoc calibrator) across datasets.

Based on these findings, we derive practical guidelines for robust calibration under shifts, visually summarised in Fig. 2. First, in terms of training strategy: the best results are obtained when classifiers are initialised with foundation model weights (as opposed to random initialisation). Then, regarding the use of in-training calibration techniques, we find that they are not needed if post-hoc calibration is used. However, if the aim is to bypass post-hoc calibration, we find in-training calibration with ER+LS to be most effective. Regarding the choice of post-hoc calibrators, we find that applying TS+OOD (or EBS) is a robust strategy for improving calibration under shifts of single classifiers (without ensembling). Finally, regarding model ensembles, we find that simply calibrating ensemble members with TS *prior* to ensembling yields robust calibration results. We find that combining this ensembling strategy with finetuning from foundation models yields the most robust calibration results overall, both ID and under shifts.

In this study, we focused exclusively on robustness of calibration under dataset shifts for image classification. It is worth noting that building reliable and well-calibrated uncertainty estimates, robust across dataset shifts, is equally relevant for other tasks. Gustafsson et al. (2023) for example studied the reliability of existing uncertainty estimates in the context of regression tasks, whereas Jorge et al. (2023) similarly studied robustness and calibration of uncertainty estimates in segmentation tasks. Moreover, the guidelines proposed here are based on our extensive evaluation of currently commonly used post-hoc and in-training calibration methods, and these may require updating as new calibration methods appear in the future. To this end, our publicly available benchmarking codebase provides a comprehensive evaluation framework and facilitates future benchmarking efforts for calibration under shifts in image classification.

Acknowledgments

M.R. is funded by an Imperial College London President's PhD Scholarship and a Google PhD Fellowship. R.M. is funded by the European Union's Horizon Europe research and innovation programme under grant agreement 101080302. B.G. and F.d.S.R. acknowledge the support of the UKRI AI programme, and the EPSRC, for CHAI - EPSRC Causality in Healthcare AI Hub (grant no. EP/Y028856/1). B.G. received support from the Royal Academy of Engineering as part of his Kheiron/RAEng Research Chair.

References

Glenn W. Brier. VERIFICATION OF FORECASTS EXPRESSED IN TERMS OF PROBABILITY. *Monthly Weather Review*, 78(1):1–3, January 1950. ISSN 1520-0493, 0027-0644. doi: 10.1175/1520-0493(1950)078<0001:VOFEIT>2.0.CO;2. URL https://journals.ametsoc.org/view/journals/mwre/78/1/1520-0493_1950_078_0001_vofeit_2_0_co_2.xml. Publisher: American Meteorological Society Section: Monthly Weather Review. (↑4)

Jacob Carse, Andres Alvarez Olmo, and Stephen McKenna. Calibration of Deep Medical Image Classifiers: Uncertainty for Safe Utilization of Machine Learning in Medical Imaging. *Uncertainty for Safe Utilization of Machine Learning in Medical Imaging*, pp. 89–99, 2022. ISSN 9783031167485. doi: 10.1007/978-3-031-16749-2_9. URL https://unsuremiccai.github.io/. Place: Switzerland Publisher: Springer Nature. (↑4)

Mircea Cimpoi, Subhransu Maji, Iasonas Kokkinos, Sammy Mohamed, and Andrea Vedaldi. Describing Textures in the Wild. In *2014 IEEE Conference on Computer Vision and Pattern Recognition*, pp. 3606–3613, June 2014. doi: 10.1109/CVPR.2014.461. URL https://ieeexplore.ieee.org/document/6909856. ISSN: 1063-6919. (↑6), (↑7)

Etienne Decencière, Xiwei Zhang, Guy Cazuguel, Bruno Lay, Béatrice Cochener, Caroline Trone, Philippe Gain, Richard Ordonez, Pascale Massin, Ali Erginay, Béatrice Charton, and Jean-Claude Klein. Feedback on a publicly distributed image database: the messidor database. *Image Analysis and Stereology*, 33(3): 231–234, August 2014. ISSN 1854-5165. doi: 10.5566/ias.1155. URL https://www.ias-iss.org/ojs/IAS/article/view/1155. Number: 3. (↑6), (↑4)

Jia Deng, Wei Dong, Richard Socher, Li-Jia Li, Kai Li, and Li Fei-Fei. ImageNet: A large-scale hierarchical image database. In *2009 IEEE Conference on Computer Vision and Pattern Recognition*, pp. 248–255, Miami, FL, June 2009. IEEE. ISBN 978-1-4244-3992-8. doi: 10.1109/CVPR.2009.5206848. URL https://ieeexplore.ieee.org/document/5206848/. (↑2)

Gianluca Detommaso, Alberto Gasparin, Andrew Wilson, and Cedric Archambeau. Uncertainty Calibration in Bayesian Neural Networks via Distance-Aware Priors, July 2022. URL http://arxiv.org/abs/2207.08200. arXiv:2207.08200 [cs, stat]. (↑4)

Alexey Dosovitskiy, Lucas Beyer, Alexander Kolesnikov, Dirk Weissenborn, Xiaohua Zhai, Thomas Unterthiner, Mostafa Dehghani, Matthias Minderer, Georg Heigold, Sylvain Gelly, Jakob Uszkoreit, and Neil Houlsby. An Image is Worth 16x16 Words: Transformers for Image Recognition at Scale. In *International Conference on Learning Representations*, October 2020. URL https://openreview.net/forum?id=YicbFdNTTy. (↑6)

Emma Dugas, Jorge Jared, and Will Cukierski. Diabetic Retinopathy Detection Kaggle Challenge, 2015. URL https://kaggle.com/competitions/diabetic-retinopathy-detection. (↑6), (↑4)

Milton Friedman. The Use of Ranks to Avoid the Assumption of Normality Implicit in the Analysis of Variance. *Journal of the American Statistical Association*, 32(200):675–701, December 1937. ISSN 0162-1459. doi: 10.1080/01621459.1937.10503522. URL https://www.tandfonline.com/doi/abs/10.1080/01621459.1937.10503522. Publisher: ASA Website. (↑10)

Miguel Fuentes, Benjamin M. Van Doren, Daniel Fink, and Daniel Sheldon. BirdFlow: Learning seasonal bird movements from eBird data. *Methods in Ecology and Evolution*, 14(3):923–938, 2023. ISSN 2041-210X. doi: 10.1111/2041-210X.14052. URL https://onlinelibrary.wiley.com/doi/abs/10.1111/2041-210X.14052. _eprint: https://onlinelibrary.wiley.com/doi/pdf/10.1111/2041-210X.14052. (↑4)

Yingbo Gao, Weiyue Wang, Christian Herold, Zijian Yang, and Hermann Ney. Towards a Better Understanding of Label Smoothing in Neural Machine Translation. In Kam-Fai Wong, Kevin Knight, and Hua Wu (eds.), *Proceedings of the 1st Conference of the Asia-Pacific Chapter of the Association for Computational Linguistics and the 10th International Joint Conference on Natural Language Processing*, pp. 212–223, Suzhou, China, December 2020. Association for Computational Linguistics. doi: 10.18653/v1/2020.aacl-main.25. URL https://aclanthology.org/2020.aacl-main.25/. (↑4)

Sebastian Gregor Gruber and Florian Buettner. Better Uncertainty Calibration via Proper Scores for Classification and Beyond. In *Advances in Neural Information Processing Systems*, October 2022. URL https://openreview.net/forum?id=PikKk2lF6P. (↑4)

Chuan Guo, Geoff Pleiss, Yu Sun, and Kilian Q. Weinberger. On Calibration of Modern Neural Networks. In *Proceedings of the 34th International Conference on Machine Learning*, pp. 1321–1330. PMLR, July 2017. URL https://proceedings.mlr.press/v70/guo17a.html. ISSN: 2640-3498. (↑1), (↑2), (↑3), (↑4), (↑6)

Kartik Gupta, Amir Rahimi, Thalaiyasingam Ajanthan, Thomas Mensink, Cristian Sminchisescu, and Richard Hartley. Calibration of Neural Networks using Splines. In *International Conference on Learning Representations*, 2021. URL https://openreview.net/forum?id=eQe8DEWNN2W. (↑2), (↑4)

Fredrik K. Gustafsson, Martin Danelljan, and Thomas B. Schön. How Reliable is Your Regression Model's Uncertainty Under Real-World Distribution Shifts? *Transactions on Machine Learning Research*, September 2023. doi: 10.48550/arXiv.2302.03679. URL https://openreview.net/forum?id=WJt2Pc3qtI. (↑14)

Kaiming He, Xiangyu Zhang, Shaoqing Ren, and Jian Sun. Deep Residual Learning for Image Recognition. In *2016 IEEE Conference on Computer Vision and Pattern Recognition (CVPR)*, pp. 770–778. IEEE, June 2016. ISBN 978-1-4673-8851-1. doi: 10.1109/CVPR.2016.90. URL http://ieeexplore.ieee.org/document/7780459/. (↑6)

Yufan He, Aaron Carass, Lianrui Zuo, Blake E. Dewey, and Jerry L. Prince. Autoencoder based self-supervised test-time adaptation for medical image analysis. *Medical Image Analysis*, 72:102136, August 2021. ISSN 1361-8415. doi: 10.1016/j.media.2021.102136. URL https://www.sciencedirect.com/science/article/pii/S1361841521001821. (↑6)

Dan Hendrycks and Thomas Dietterich. Benchmarking Neural Network Robustness to Common Corruptions and Perturbations. In *International Conference on Learning Representations*, September 2018. URL https://openreview.net/forum?id=HJz6tiCqYm. (↑2), (↑5)

Andrew G. Howard, Menglong Zhu, Bo Chen, Dmitry Kalenichenko, Weijun Wang, Tobias Weyand, Marco Andreetto, and Hartwig Adam. MobileNets: Efficient Convolutional Neural Networks for Mobile Vision Applications, April 2017. URL http://arxiv.org/abs/1704.04861. arXiv:1704.04861 [cs]. (↑6)

Jeremy Irvin, Pranav Rajpurkar, Michael Ko, Yifan Yu, Silviana Ciurea-Ilcus, Chris Chute, Henrik Marklund, Behzad Haghgoo, Robyn Ball, Katie Shpanskaya, Jayne Seekins, David A. Mong, Safwan S. Halabi, Jesse K. Sandberg, Ricky Jones, David B. Larson, Curtis P. Langlotz, Bhavik N. Patel, Matthew P. Lungren, and Andrew Y. Ng. CheXpert: a large chest radiograph dataset with uncertainty labels and expert comparison. In *Proceedings of the Thirty-Third AAAI Conference on Artificial Intelligence and Thirty-First Innovative Applications of Artificial Intelligence Conference and Ninth AAAI Symposium on Educational Advances in Artificial Intelligence*, AAAI'19/IAAI'19/EAAI'19, pp. 590–597, Honolulu, Hawaii, USA, January 2019. AAAI Press. ISBN 978-1-57735-809-1. doi: 10.1609/aaai.v33i01.3301590. URL https://doi.org/10.1609/aaai.v33i01.3301590. (↑6), (↑4)

Jiwoong J. Jeong, Brianna L. Vey, Ananth Bhimireddy, Thomas Kim, Thiago Santos, Ramon Correa, Raman Dutt, Marina Mosunjac, Gabriela Oprea-Ilies, Geoffrey Smith, Minjae Woo, Christopher R. McAdams, Mary S. Newell, Imon Banerjee, Judy Gichoya, and Hari Trivedi. The EMory BrEast imaging Dataset (EMBED): A Racially Diverse, Granular Dataset of 3.4 Million Screening and Diagnostic Mammographic Images. *Radiology: Artificial Intelligence*, 5(1):e220047, January 2023. doi: 10.1148/ryai.220047. URL https://pubs.rsna.org/doi/10.1148/ryai.220047. Publisher: Radiological Society of North America. (↑5), (↑1)

Alistair E. W. Johnson, Tom J. Pollard, Seth J. Berkowitz, Nathaniel R. Greenbaum, Matthew P. Lungren, Chih-ying Deng, Roger G. Mark, and Steven Horng. MIMIC-CXR, a de-identified publicly available database of chest radiographs with free-text reports. *Scientific Data*, 6(1):317, December 2019. ISSN 2052-4463. doi: 10.1038/s41597-019-0322-0. URL https://www.nature.com/articles/s41597-019-0322-0. Publisher: Nature Publishing Group. (↑6), (↑4)

Pau de Jorge, Riccardo Volpi, Philip Torr, and Gregory Rogez. Reliability in Semantic Segmentation: Are We on the Right Track?, March 2023. URL http://arxiv.org/abs/2303.11298. arXiv:2303.11298 [cs]. (↑14)

Maggie Karthik and Dane Sohier. APTOS 2019 Blindness Detection Kaggle Challenge, 2019. URL https://kaggle.com/competitions/aptos2019-blindness-detection. (↑6), (↑4)

Mijoo Kim and Junseok Kwon. Uncertainty Calibration with Energy Based Instance-Wise Scaling in the Wild Dataset. In Aleš Leonardis, Elisa Ricci, Stefan Roth, Olga Russakovsky, Torsten Sattler, and Gül Varol (eds.), *European Conference on Computer Vision*, volume 15104 of *Lecture Notes in Computer Science*, pp. 232–248, Cham, 2024. Springer Nature Switzerland. ISBN 978-3-031-72952-2. doi: 10.1007/978-3-031-72952-2_14. URL https://arxiv.org/abs/2407.12330. (↑2), (↑3), (↑5), (↑6), (↑7)

Pang Wei Koh, Shiori Sagawa, Henrik Marklund, Sang Michael Xie, Marvin Zhang, Akshay Balsubramani, Weihua Hu, Michihiro Yasunaga, Richard Lanas Phillips, Irena Gao, Tony Lee, Etienne David, Ian Stavness, Wei Guo, Berton Earnshaw, Imran Haque, Sara M. Beery, Jure Leskovec, Anshul Kundaje, Emma Pierson, Sergey Levine, Chelsea Finn, and Percy Liang. WILDS: A Benchmark of in-the-Wild Distribution Shifts. In *Proceedings of the 38th International Conference on Machine Learning*, pp. 5637–5664. PMLR, July 2021. URL https://proceedings.mlr.press/v139/koh21a.html. ISSN: 2640-3498. (↑2), (↑5), (↑6), (↑4)

Alex Krizhevsky. Learning Multiple Layers of Features from Tiny Images. Technical report, University of Toronto, 2009. (↑2)

Ananya Kumar, Tengyu Ma, Percy Liang, and Aditi Raghunathan. Calibrated ensembles can mitigate accuracy tradeoffs under distribution shift. In *Proceedings of the Thirty-Eighth Conference on Uncertainty in Artificial Intelligence*, pp. 1041–1051. PMLR, August 2022. URL https://proceedings.mlr.press/v180/kumar22a.html. ISSN: 2640-3498. (↑3), (↑5)

Balaji Lakshminarayanan, Alexander Pritzel, and Charles Blundell. Simple and Scalable Predictive Uncertainty Estimation using Deep Ensembles. In *Advances in Neural Information Processing Systems*, volume 30. Curran Associates, Inc., 2017. URL https://proceedings.neurips.cc/paper_files/paper/2017/hash/9ef2ed4b7fd2c810847ffa5fa85bce38-Abstract.html. (↑3), (↑4), (↑5), (↑13)

Tsung-Yi Lin, Priya Goyal, Ross Girshick, Kaiming He, and Piotr Dollár. Focal Loss for Dense Object Detection. *IEEE Transactions on Pattern Analysis and Machine Intelligence*, 42(2):318–327, February 2020. ISSN 1939-3539. doi: 10.1109/TPAMI.2018.2858826. URL https://ieeexplore.ieee.org/document/8417976/?arnumber=8417976. Conference Name: IEEE Transactions on Pattern Analysis and Machine Intelligence. (↑4)

Zhuang Liu, Hanzi Mao, Chao-Yuan Wu, Christoph Feichtenhofer, Trevor Darrell, and Saining Xie. A ConvNet for the 2020s. In *2022 IEEE/CVF Conference on Computer Vision and Pattern Recognition (CVPR)*, pp. 11966–11976, New Orleans, LA, USA, June 2022. IEEE. ISBN 978-1-66546-946-3. doi: 10.1109/CVPR52688.2022.01167. URL https://ieeexplore.ieee.org/document/9879745/. (↑4), (↑6)

Laurens van der Maaten and Geoffrey Hinton. Visualizing Data using t-SNE. *Journal of Machine Learning Research*, 9(86):2579–2605, 2008. ISSN 1533-7928. URL http://jmlr.org/papers/v9/vandermaaten08a.html. (↑8)

Wesley J Maddox, Pavel Izmailov, Timur Garipov, Dmitry P Vetrov, and Andrew Gordon Wilson. A Simple Baseline for Bayesian Uncertainty in Deep Learning. In *Advances in Neural Information Processing Systems*, volume 32. Curran Associates, Inc., 2019. URL https://proceedings.neurips.cc/paper/2019/hash/118921efba23fc329e6560b27861f0c2-Abstract.html. (↑4)

Raghav Mehta, Vítor Albiero, Li Chen, Ivan Evtimov, Tamar Glaser, Zhiheng Li, and Tal Hassner. You Only Need a Good Embeddings Extractor to Fix Spurious Correlations, December 2022. URL http://arxiv.org/abs/2212.06254. arXiv:2212.06254 [cs]. (↑3)

Clara Meister, Elizabeth Salesky, and Ryan Cotterell. Generalized Entropy Regularization or: There's Nothing Special about Label Smoothing, May 2020. URL http://arxiv.org/abs/2005.00820. arXiv:2005.00820 [cs]. (↑2), (↑4)

Jishnu Mukhoti, Viveka Kulharia, Amartya Sanyal, Stuart Golodetz, Philip Torr, and Puneet Dokania. Calibrating Deep Neural Networks using Focal Loss. In *Advances in Neural Information Processing Systems*, volume 33, pp. 15288–15299. Curran Associates, Inc., 2020. URL https://proceedings.neurips.cc/paper/2020/hash/aeb7b30ef1d024a76f21a1d40e30c302-Abstract.html. (↑2), (↑4)

Kevin P. Murphy. *Probabilistic machine learning: advanced topics*. Adaptive computation and machine learning series. The MIT Press, Cambridge, Massachusetts, 2023. ISBN 978-0-262-37599-3 978-0-262-37600-6. (↑1)

Rafael Müller, Simon Kornblith, and Geoffrey Hinton. When does label smoothing help? In *Proceedings of the 33rd International Conference on Neural Information Processing Systems*, pp. 4694–4703, Red Hook, NY, USA, December 2019. Curran Associates Inc. (↑2), (↑4)

Peter Nemenyi. *Distribution-free Multiple Comparisons*. Princeton University, 1963. (↑10)

Jeremy Nixon, Michael W Dusenberry, Linchuan Zhang, Ghassen Jerfel, and Dustin Tran. Measuring Calibration in Deep Learning. In *Proceedings of the IEEE/CVF Conference on Computer Vision and Pattern Recognition (CVPR) Workshops*, pp. 38–41, 2019. (↑4)

Maxime Oquab, Timothée Darcet, Théo Moutakanni, Huy V. Vo, Marc Szafraniec, Vasil Khalidov, Pierre Fernandez, Daniel Haziza, Francisco Massa, Alaaeldin El-Nouby, Mido Assran, Nicolas Ballas, Wojciech Galuba, Russell Howes, Po-Yao Huang, Shang-Wen Li, Ishan Misra, Michael Rabbat, Vasu Sharma, Gabriel Synnaeve, Hu Xu, Herve Jegou, Julien Mairal, Patrick Labatut, Armand Joulin, and Piotr Bojanowski. DINOv2: Learning Robust Visual Features without Supervision. *Transactions on Machine Learning Research*, July 2023. ISSN 2835-8856. URL https://openreview.net/forum?id=a68SUt6zFt. (↑3), (↑6)

Yaniv Ovadia, Emily Fertig, Jie Ren, Zachary Nado, D. Sculley, Sebastian Nowozin, Joshua Dillon, Balaji Lakshminarayanan, and Jasper Snoek. Can you trust your model' s uncertainty? Evaluating predictive uncertainty under dataset shift. In *Advances in Neural Information Processing Systems*, volume 32. Curran Associates, Inc., 2019. URL https://proceedings.neurips.cc/paper/2019/hash/8558cb408c1d76621371888657d2eb1d-Abstract.html. (↑2), (↑5)

Xingchao Peng, Qinxun Bai, Xide Xia, Zijun Huang, Kate Saenko, and Bo Wang. Moment Matching for Multi-Source Domain Adaptation. In *2019 IEEE/CVF International Conference on Computer Vision (ICCV)*, pp. 1406–1415, Seoul, Korea (South), October 2019. IEEE. ISBN 978-1-72814-803-8. doi: 10.1109/ICCV.2019.00149. URL https://ieeexplore.ieee.org/document/9010750/. (↑6), (↑4)

Gabriel Pereyra, George Tucker, Jan Chorowski, Lukasz Kaiser, and Geoffrey Hinton. Regularizing Neural Networks by Penalizing Confident Output Distributions. In *International Conference on Learning Representations*, February 2017. URL https://openreview.net/forum?id=HyhbYrGYe. (↑2), (↑4)

Alec Radford, Jong Wook Kim, Chris Hallacy, Aditya Ramesh, Gabriel Goh, Sandhini Agarwal, Girish Sastry, Amanda Askell, Pamela Mishkin, Jack Clark, Gretchen Krueger, and Ilya Sutskever. Learning Transferable Visual Models From Natural Language Supervision. In *Proceedings of the 38th International Conference on Machine Learning*, pp. 8748–8763. PMLR, July 2021. URL https://proceedings.mlr.press/v139/radford21a.html. ISSN: 2640-3498. (↑6)

Rahul Rahaman and Alexandre Thiery. Uncertainty Quantification and Deep Ensembles. In *Advances in Neural Information Processing Systems*, volume 34, pp. 20063–20075. Curran Associates, Inc., 2021. URL https://proceedings.neurips.cc/paper_files/paper/2021/hash/a70dc40477bc2adceef4d2c90f47eb82-Abstract.html. (↑3), (↑5), (↑13)

Shibani Santurkar, Dimitris Tsipras, and Aleksander Madry. BREEDS: Benchmarks for Subpopulation Shift. In *International Conference on Learning Representations*, October 2020. URL https://openreview.net/forum?id=mQPBmvyAuk. (↑5)

Florian Seligmann, Philipp Becker, Michael Volpp, and Gerhard Neumann. Beyond Deep Ensembles: A Large-Scale Evaluation of Bayesian Deep Learning under Distribution Shift. In *Thirty-seventh Conference on Neural Information Processing Systems*, November 2023. URL https://openreview.net/forum?id=jX49iKr6vb&noteId=0j4MnXsU53. (↑2), (↑3), (↑4), (↑5)

Congzhen Shi, Ryan Rezai, Jiaxi Yang, Qi Dou, and Xiaoxiao Li. A Survey on Trustworthiness in Foundation Models for Medical Image Analysis, October 2024. URL http://arxiv.org/abs/2407.15851. arXiv:2407.15851. (↑3)

Christian Szegedy, Vincent Vanhoucke, Sergey Ioffe, Jon Shlens, and Zbigniew Wojna. Rethinking the Inception Architecture for Computer Vision. In *2016 IEEE Conference on Computer Vision and Pattern Recognition (CVPR)*, pp. 2818–2826, June 2016. doi: 10.1109/CVPR.2016.308. URL https://ieeexplore.ieee.org/document/7780677/?arnumber=7780677. ISSN: 1063-6919. (↑2), (↑3), (↑4)

Mingxing Tan and Quoc Le. EfficientNet: Rethinking Model Scaling for Convolutional Neural Networks. In *Proceedings of the 36th International Conference on Machine Learning*, pp. 6105–6114. PMLR, May 2019. URL https://proceedings.mlr.press/v97/tan19a.html. ISSN: 2640-3498. (↑6)

Rohan Taori, Achal Dave, Vaishaal Shankar, Nicholas Carlini, Benjamin Recht, and Ludwig Schmidt. Measuring Robustness to Natural Distribution Shifts in Image Classification. In *Advances in Neural Information Processing Systems*, volume 33, pp. 18583–18599. Curran Associates, Inc., 2020. URL https://proceedings.neurips.cc/paper/2020/hash/d8330f857a17c53d217014ee776bfd50-Abstract.html. (↑2)

Christian Tomani, Sebastian Gruber, Muhammed Ebrar Erdem, Daniel Cremers, and Florian Buettner. Post-Hoc Uncertainty Calibration for Domain Drift Scenarios. In *Proceedings of the IEEE/CVF Conference on Computer Vision and Pattern Recognition*, pp. 10124–10132, 2021. URL https://openaccess.thecvf.com/content/CVPR2021/html/Tomani_Post-Hoc_Uncertainty_Calibration_for_Domain_Drift_Scenarios_CVPR_2021_paper.html. (↑2), (↑5), (↑6)

Christian Tomani, Futa Kai Waseda, Yuesong Shen, and Daniel Cremers. Beyond In-Domain Scenarios: Robust Density-Aware Calibration. In *Proceedings of the 40th International Conference on Machine Learning*, pp. 34344–34368. PMLR, July 2023. URL https://proceedings.mlr.press/v202/tomani23a.html. ISSN: 2640-3498. (↑2), (↑5)

Cheng Wang, Jorge Balazs, György Szarvas, Patrick Ernst, Lahari Poddar, and Pavel Danchenko. Calibrating Imbalanced Classifiers with Focal Loss: An Empirical Study. In Yunyao Li and Angeliki Lazaridou (eds.), *Proceedings of the 2022 Conference on Empirical Methods in Natural Language Processing: Industry Track*, pp. 145–153, Abu Dhabi, UAE, December 2022. Association for Computational Linguistics. doi: 10.18653/v1/2022.emnlp-industry.14. URL https://aclanthology.org/2022.emnlp-industry.14/. (↑4)

Deng-Bao Wang, Lei Feng, and Min-Ling Zhang. Rethinking Calibration of Deep Neural Networks: Do Not Be Afraid of Overconfidence. In *Advances in Neural Information Processing Systems*, volume 34, pp. 11809–11820. Curran Associates, Inc., 2021. URL https://proceedings.neurips.cc/paper/2021/hash/61f3a6dbc9120ea78ef75544826c814e-Abstract.html. (↑3)

Jerry Wei, Lorenzo Torresani, Jason Wei, and Saeed Hassanpour. Calibrating Histopathology Image Classifiers Using Label Smoothing. In Martin Michalowski, Syed Sibte Raza Abidi, and Samina Abidi (eds.), *Artificial Intelligence in Medicine*, pp. 273–282, Cham, 2022. Springer International Publishing. ISBN 978-3-031-09342-5. doi: 10.1007/978-3-031-09342-5_26. (↑4)

Xixin Wu and Mark Gales. Should Ensemble Members Be Calibrated?, January 2021. URL http://arxiv.org/abs/2101.05397. arXiv:2101.05397 [cs]. (↑5)

Yaodong Yu, Yi Ma, Stephen Bates, and Michael I Jordan. Robust Calibration with Multi-domain Temperature Scaling. In *Advances in Neural Information Processing Systems*, 2022. (↑5)

Mert Yuksekgonul, Linjun Zhang, James Zou, and Carlos Guestrin. Beyond Confidence: Reliable Models Should Also Consider Atypicality. In *Advances in Neural Information Processing Systems*, November 2023. URL https://openreview.net/forum?id=ZVRG3toCTT&noteId=w31lGzmi0V. (↑2), (↑5)

Bianca Zadrozny and Charles Elkan. Transforming classifier scores into accurate multiclass probability estimates. In *Proceedings of the eighth ACM SIGKDD international conference on Knowledge discovery and data mining*, KDD '02, pp. 694–699, New York, NY, USA, July 2002. Association for Computing Machinery. ISBN 978-1-58113-567-1. doi: 10.1145/775047.775151. URL https://doi.org/10.1145/775047.775151. (↑2), (↑4), (↑6)

Xiaohua Zhai, Basil Mustafa, Alexander Kolesnikov, and Lucas Beyer. Sigmoid Loss for Language Image Pre-Training. In *2023 IEEE/CVF International Conference on Computer Vision (ICCV)*, pp. 11941–11952, Paris, France, October 2023. IEEE. ISBN 9798350307184. doi: 10.1109/ICCV51070.2023.01100. URL https://ieeexplore.ieee.org/document/10377550/. (↑6)

Jize Zhang, Bhavya Kailkhura, and T. Yong-Jin Han. Mix-n-Match : Ensemble and Compositional Methods for Uncertainty Calibration in Deep Learning. In *Proceedings of the 37th International Conference on Machine Learning*, pp. 11117–11128. PMLR, November 2020. URL https://proceedings.mlr.press/v119/zhang20k.html. ISSN: 2640-3498. (↑2), (↑3), (↑4), (↑6)

Jun Zhang, Wen Yao, Xiaoqian Chen, and Ling Feng. Understanding Negative Calibration from Entropy Perspective. In Michelangelo Ceci, Sergio Flesca, Elio Masciari, Giuseppe Manco, and Zbigniew W. Raś (eds.), *Foundations of Intelligent Systems*, volume 13515, pp. 305–314. Springer International Publishing, Cham, 2022. ISBN 978-3-031-16563-4 978-3-031-16564-1. doi: 10.1007/978-3-031-16564-1_29. URL https://link.springer.com/10.1007/978-3-031-16564-1_29. Series Title: Lecture Notes in Computer Science. (↑3), (↑5)

Sheng Zhang, Yanbo Xu, Naoto Usuyama, Hanwen Xu, Jaspreet Bagga, Robert Tinn, Sam Preston, Rajesh Rao, Mu Wei, Naveen Valluri, Cliff Wong, Andrea Tupini, Yu Wang, Matt Mazzola, Swadheen Shukla, Lars Liden, Jianfeng Gao, Angela Crabtree, Brian Piening, Carlo Bifulco, Matthew P. Lungren, Tristan Naumann, Sheng Wang, and Hoifung Poon. A Multimodal Biomedical Foundation Model Trained from Fifteen Million Image–Text Pairs. *NEJM AI*, 2(1):AIoa2400640, January 2025. doi: 10.1056/AIoa2400640. URL https://ai.nejm.org/doi/full/10.1056/AIoa2400640. Publisher: Massachusetts Medical Society. (↑3), (↑6)

Yukun Zhou, Mark A. Chia, Siegfried K. Wagner, Murat S. Ayhan, Dominic J. Williamson, Robbert R. Struyven, Timing Liu, Moucheng Xu, Mateo G. Lozano, Peter Woodward-Court, Yuka Kihara, Andre Altmann, Aaron Y. Lee, Eric J. Topol, Alastair K. Denniston, Daniel C. Alexander, and Pearse A. Keane. A foundation model for generalizable disease detection from retinal images. *Nature*, 622(7981):156–163, October 2023. ISSN 1476-4687. doi: 10.1038/s41586-023-06555-x. URL https://www.nature.com/articles/s41586-023-06555-x. Publisher: Nature Publishing Group. (↑3)

A.1 Dataset definitions

In this work we study realistic shifts in the medical imaging and natural images domain. For this we leverage multiple public datasets across various modalities and tasks. We here detail how we defined ID and OOD domains for non-standard benchmark datasets. We summarise splits and ID/shifted domains definitions in Table A.1. In Figs. A.1 and A.2 we illustrate the types of shift by showing examples of images from both the ID and the shifted sets for each dataset.

Dataset	Type of shift(s)	N classes Balanced (Y/N)	ID domain ($N_{train}, N_{val}, N_{test}$)	Shifted domains (N images)
CXR	Scanner Prevalence Population	2 classes (N)	CheXpert random train/val/test split (129732, 23086, 38192)	MIMIC-CXR random subset (25000)
RETINA	Scanner Prevalence Population	5 classes (N)	EyePACS (35126, 10715, 42861)	Messidor (1744) Aptos (3662)
EMBED	Scanner	4 classes (N)	Selenia Dimension 2D (169758, 43055, 52975)	Senographe Essential (12218) Senograph 2000D (13268) Lorad Selenia (10515) Senographe Pristina (498) Clearview CSm (8128) Selenia Dimensions C-views (108369)
CameLyon	Staining	2 classes (Y)	Official ID splits Hospitals 1,2,3 (272192, 30244, 33560)	Official OOD splits Hospital 4 (34904) Hospital 5 (85054)
iCam	Geographic Prevalence	182 classes (N)	Official ID splits (129809, 7314, 8154)	'OOD val' split (14961) 'OOD test' split (42791)
Living17	Population	17 classes (Y)	Source domain from official 'rand' split (37570, 6630, 1700)	Target test set from official 'rand' split (1700)
Entity30	Population	30 classes (Y)	Source domain from official 'rand' split (131123, 23140, 6000)	Target test set from official 'rand' split (6000)
DomainNet	Image type Prevalence	345 classes (N)	Official ID splits from Wilds with ID domain 'Real' (217630, 24182, 104082)	Clipart test (14604) Infograph test (15582) Painting test (21850) Quickdraw test (51750) Sketch test (20916)

Table A.1: Datasets and shifts used in this study, details on ID and shifted splits definition.

EMBED we analyse robustness against scanner changes for breast density assessment models in mammography. For this purpose, we use the public available EMBED dataset (Jeong et al., 2023). This dataset contains data from 6 different scanners (Selenia Dimensions, Senographe Essential, Senograph 2000D, Lorad Selenia, Clearview CSm, Senographe Pristina). In this work, we used Selenia Dimensions (2D images) as the ID scanner for training and validation, and all the other scanners, as well as the C-view images from Selenia Dimensions, are used as shifted test sets, resulting in six shifted test sets.

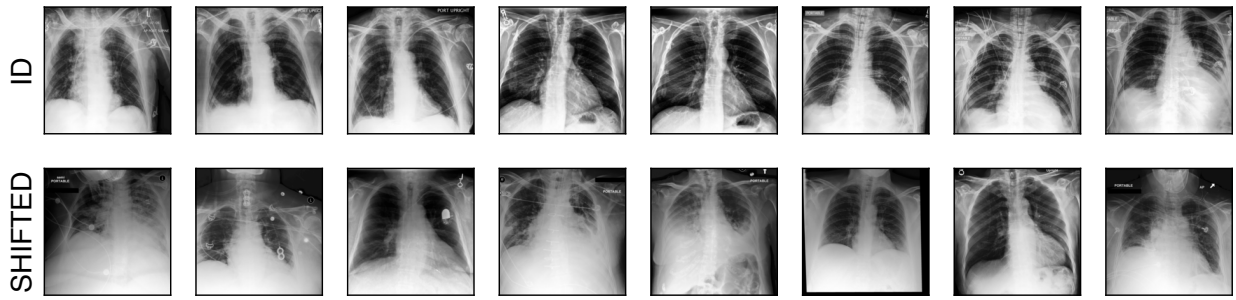

(a) CXR

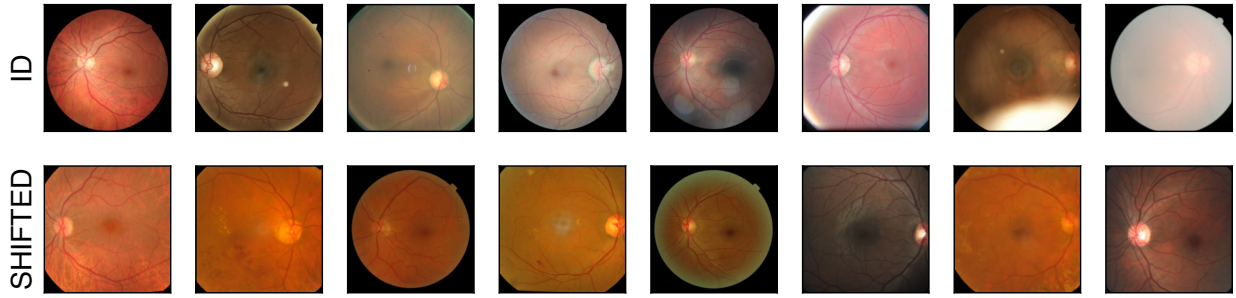

(b) RETINA

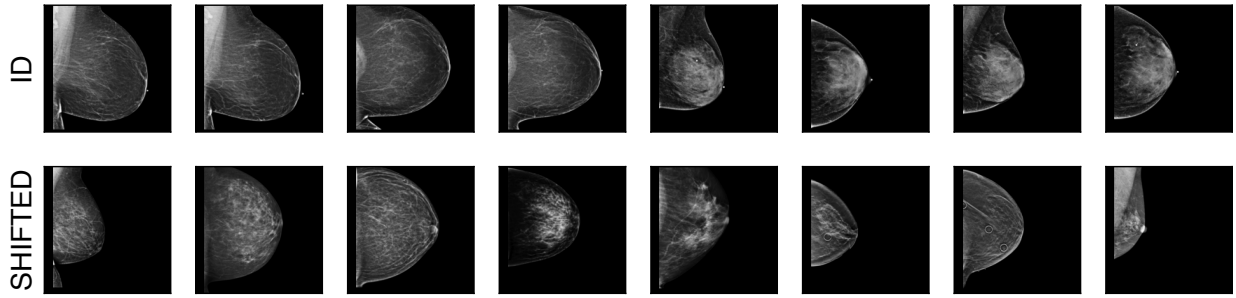

(c) EMBED

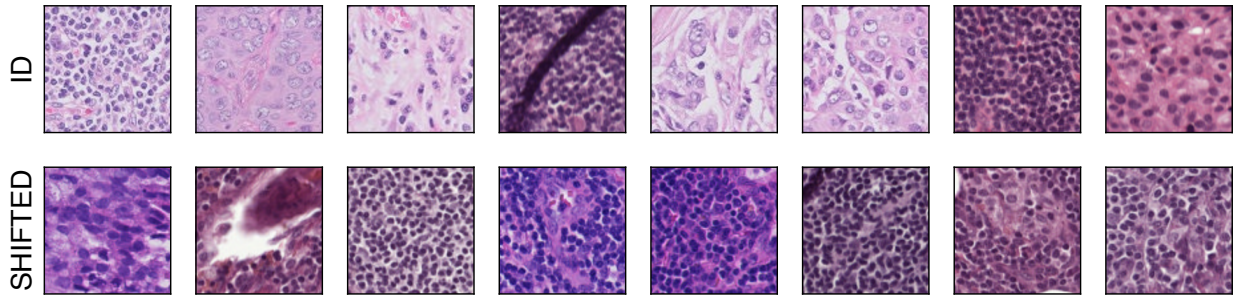

(d) CameLyon

Figure A.1: Illustration of each dataset and associated shifts (1/2).

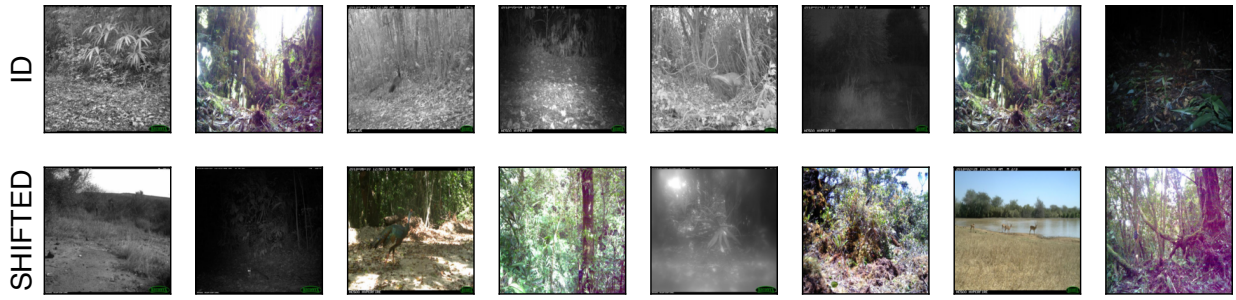

(a) iCam

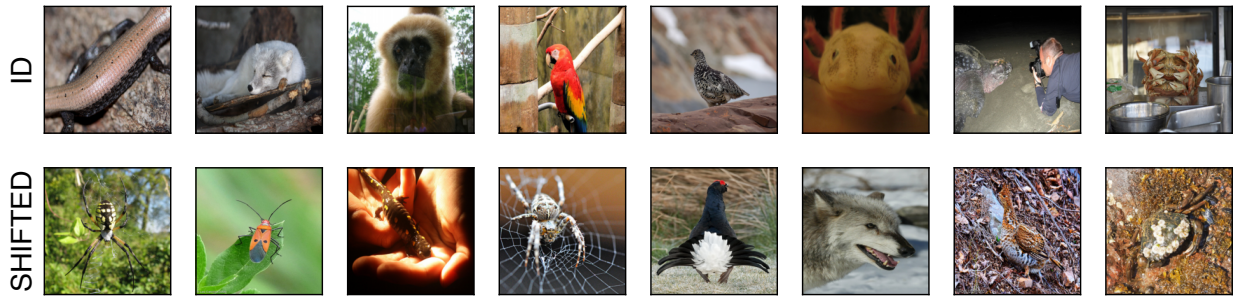

(b) Living17



(c) DomainNet

Figure A.2: Illustration of each dataset and associated shifts (2/2).

RETINA we analyse robustness against equipment and geographic location changes in diabetic retinopathy grading models by combining three publicly available datasets: Kaggle Diabetic Retinopathy Challenge (EyePACS) dataset (Dugas et al., 2015), Kaggle Aptos dataset (Karthik & Sohier, 2019) and the Messidor-v2 (Decencière et al., 2014) dataset. These datasets cover various locations (US, India and France) and different level of equipment from high-quality scanners to mobile phone cameras. We use the largest dataset (EyePACS) as ID domain, and images from the two other datasets as OOD test sets.

CXR we analyse robustness against scanner, location and label distribution changes in chest-xray classification models (No Finding versus Disease task) using the CheXpert (Irvin et al., 2019) and MIMIC-CXR (Johnson et al., 2019) datasets. We use the CheXpert dataset as our ID domain, splitting randomly between train/val/test at the patient level, and we use a random subset of 25,000 images from the MIMIC-CXR database as our OOD test set.

DomainNet we use the implementation and splits definition provided by the Wilds package (Koh et al., 2021) for our DomainNet (Peng et al., 2019) experiments. Specifically, we use images from the 'REAL' domain as our ID images (train/test/test), and images from all other 5 domains (clipart, infograph, painting, quickdraw, sketch).

A.2 Details on calibration metrics computation

Expected Calibration Error, or ECE (Guo et al., 2017) approximates the expected difference between predicted confidence and prediction accuracy. We follow the notations from the main paper: with a classification task with C classes, $x \in \mathcal{X}$ the model input, and $y \in \{1, \dots, C\}$ the associated label. Let $\hat{\mathbf{p}} \in [0,1]^C$ denote the model predicted probabilities for each class, $\hat{y} = \arg\max_i \hat{p}_i$ the predicted class, and $\hat{c} = \max \hat{p}_i$ the associated confidence score. To compute ECE, the output space $[0,1]$ is partitioned into M bins, for each bin B_m, we compute the average confidence score in the bin $\text{Conf}(B_m) = \frac{1}{|B_m|} \sum_{\hat{c}^i \in B_m} \hat{c}^i$ and the actual accuracy in this bin $\text{Acc}(B_m) = \frac{1}{|B_m|} \sum_{\hat{c}^i \in B_m} \mathbb{1}[y^i = \hat{y}^i]$. The ECE then reflects the average error over all bins, weighted by the number of samples in each bin:

$$ECE = \sum_{m=1}^{M} \frac{|B_m|}{N} \left|\text{Acc}(B_m) - \text{Conf}(B_m)\right| \tag{1}$$

with N the total number of samples.

The Brier Score (Brier, 1950), on the other hand computes the average class-wise mean squared error between probabilities and one-hot labels. Formally, the score is computed as: $\frac{1}{N} \sum_{i=1}^{N} \sum_{k=1}^{C} \left(\hat{p}_k^i - y_k^i\right)^2$.

A.3 Comparison with existing studies

For the convenience of the reader, below we provide a comparative table summarising differences between previous studies on calibration under shifts in image classification and our study.

Paper	Datasets	Type of shifts	Post-hoc methods	In-training calibration methods	Bayesian approaches	Effect of ensembling	Effect of foundation models
Ovadia et al. (2019)	Rotated MNIST, Translated MNIST, CIFAR10-C, ImageNet-C	Synthetic	TS	-	✓	✓	-
Tomani et al. (2021)	CIFAR10-C, ImageNet-C, ObjectNet	Synthetic	TS, IR, IRM, TS-IR with(out) perturbation on val set	-	-	-	-
Tomani et al. (2023)	CIFAR10-C, CIFAR100-C, ImageNet-C	Synthetic	TS, ETS, IRM, SPL with(out) DAC	-	-	-	-
Kim & Kwon (2024)	CIFAR10-C, CIFAR100-C, ImageNet-C	Synthetic	ETS, SPLINE, EBS, IRM, IROVa, IROVaTS, DAC	-	-	-	-
Yu et al. (2022)	ImageNet-C, WILDS-RxRx1, GLDv2	Synthetic + Real-world	TS, MD+TS	-	-	-	-
Kumar et al. (2022)	Cropland, Landcover, CelebA, Living17, Entity30, DomainNet, ImageNet, iWildCam, Waterbirds	Real-world	TS	-	✓	-	
Zhang et al. (2022)	CIFAR10-C, CIFAR100-C, TinyImageNet-C	Synthetic	TS	LS, Focal	-	-	-
Seligmann et al. (2023)	WiLDS datasets (iCAM, FMoW, RxRx1), CIFAR10-C,	Synthetic + Real-world	-	-	✓	✓ for BNNs	-
Ours	WiLDS datasets (iCam, CameLyon), Living17, Entity30, EMBED, CheXpert, MIMIC-CXR, RETINA, DomainNet	Real-world	TS (+OOD), IROVaTS (+OOD), IRM (+OOD), EBS	LS, ER, ER+LS, focal	-	✓	✓

Table A.2: Comparison of our and other existing studies on calibration under dataset shifts in image classification, see Section 2 for more details.

Dataset	LR schedule for CNNs	LR schedule for ViT	LR schedule for ConvNext	Max epochs
Living17	Cosine 10^{-3} to 10^{-5}	Fixed 10^{-5}	Fixed 10^{-4}	50
Entity30	Cosine 10^{-3} to 10^{-5}	Fixed 10^{-5}	Fixed 10^{-4}	100
CXR	Cosine 10^{-4} to 10^{-5}	Fixed 10^{-5}	Fixed 10^{-4}	50
Density	Cosine 10^{-4} to 10^{-5}	Fixed 10^{-5}	Fixed 10^{-4}	50
iCam	Cosine 10^{-4} to 10^{-5}	Fixed 10^{-5}	Fixed 10^{-4}	100
RETINA	Cosine 10^{-3} to 10^{-5}	Fixed 10^{-5}	Fixed 10^{-4}	150
DomainNet	Cosine 10^{-3} to 10^{-5}	Fixed 10^{-5}	Fixed 10^{-4}	150
CameLyon	Cosine 10^{-3} to 10^{-5}	Fixed 10^{-5}	Fixed 10^{-4}	150

Table A.3: Learning rate schedules used to train models initialised with random weights, per dataset. Learning rate schedules were chosen based on best validation performance.

A.4 Hyperparameters and training setup details

All of our classification models were trained using a standard cross-entropy loss, using the Adam optimiser, with a batch size of 32. For models trained from scratch, we used a cosine learning rate schedule or a fixed learning rate schedule, depending on the architecture and the dataset, chosen based on validation performance, we detail all configurations in Table A.3. For finetuning foundation models, we used a fixed learning rate of 10^{-5}, chosen based on validation performance. We performed full-finetuning of foundation models, i.e. all weights were finetuned. For all experiments, we chose the checkpoint with the highest validation balanced accuracy for inference.

A.5 Post-hoc calibrators with semantic OOD exposure: implementation details

A.5.1 EBS: Energy-based calibration, implementation details

In this section, we detail the algorithm proposed by Kim & Kwon (2024) for their energy-based calibration method.

Algorithm 1: Energy-based calibration (Kim & Kwon, 2024)

Input: In-distribution dataset: $\mathcal{D}_{id} = \{(\mathbf{x}_i, y_i)\}_{i=1}^{N}$
Input: Classifier $f(\mathbf{x})$
Input: Semantic OOD data: $\mathcal{D}_{out} = \{(\tilde{\mathbf{x}}_i, 0^C)\}_{i=1}^{N_{ood}}$
Input: Temperature value from temperature scaling: T_{ts}
`/* Get energy for all samples */`
$\mathcal{D} \leftarrow \mathcal{D}_{id} \cup \mathcal{D}_{out}$
$\mathbf{z} \leftarrow f(\mathbf{x})$
$\mathcal{F}(\mathbf{z}) \leftarrow -\texttt{logsumexp}(\mathbf{z})$
`/* Estimate Gaussian PDFs on correctly classified samples */`
$P_1 \leftarrow \text{fit}(\mathcal{F}(\mathbf{z}_{\text{correct}}))$
`/* Estimate Gaussian PDFs on incorrect + OOD samples */`
$P_2 \leftarrow \text{fit}(\mathcal{F}(\mathbf{z}_{\text{incorrect}}))$
`/* Fit calibrator */`
$T(\mathbf{z}_i) \leftarrow T_{ts} - P_1(\mathcal{F}(\mathbf{z}_i))\theta_1 + P_2(\mathcal{F}(\mathbf{z}_i))\theta_2$
$\hat{\theta} \leftarrow \arg\min_\theta \sum_{i \in \mathcal{D}} \texttt{MSE}(\texttt{softmax}(\mathbf{z}_i / T(\mathbf{z}_i)), y_i)$
Output: $\hat{\theta}, T_{ts}, P_1, P_2$

A.5.2 Enhancing other calibrators with OOD exposure

EBS (Kim & Kwon, 2024) requires exposure to a small 'semantic OOD' set for calibration, unrelated to the task at hand. Kim & Kwon (2024) propose to use samples from the Textures (Cimpoi et al., 2014) dataset as OOD samples. To disentangle the contribution of the energy-based calibration approach and the use of semantic OOD towards improved calibration, in this study we evaluate augmented versions of 'standard' post-hoc calibrators, where the same semantic OOD set is used along the ID calibration set in the calibration stage, yielding additional calibrators **TS + OOD**, **IRM + OOD**, **IROVaTS + OOD**. Concretely, we collect an unlabeled sample of OOD data and combine it with the ID calibration set to fit the calibrator of choice. For the calibration set, labels need to be assigned to the OOD samples, in this case we simply assign the uniform distribution i.e. for all samples $y = [1/C, ..., 1/C]$ where C is the number of classes. We illustrate the full process for the example of temperature scaling with OOD, in Algorithm 2. For any other calibrator (IRM, IROVaTS) the process is identical, only the fit step needs to be adapted.

Algorithm 2: Temperature scaling with semantic OOD

Input: In-distribution dataset: $\mathcal{D}_{id} = \{(\mathbf{x}_i, y_i)\}_{i=1}^{N}$

Input: Classifier $f(\mathbf{x})$

Input: Semantic OOD data: $\mathcal{D}_{out} = \{\tilde{\mathbf{x}}_i\}_{i=1}^{N_{ood}}$

`/* Assign uniform distribution as labels for OOD samples */`

for $i = 1 \rightarrow N_{ood}$ **do**

$\quad \tilde{y}_i \leftarrow \frac{1}{C} \cdot \mathbf{1}_C$

end

$\mathcal{D}_{out} \leftarrow \{(\tilde{\mathbf{x}}_i, \tilde{y}_i)\}_{i=1}^{N_{ood}}$

`/* Combine both datasets */`

$\mathcal{D} \leftarrow \mathcal{D}_{id} \cup \mathcal{D}_{out}$

`/* Fit calibrator on the combined dataset, here TS */`

$\hat{T} \leftarrow \arg\min_T \sum_{(\mathbf{x},y)\in\mathcal{D}} \text{CrossEntropy}(\texttt{softmax}(f(\mathbf{x})/T), y)$

Output: $\hat{T}$

A.5.3 Ablation study: embedding space analysis between ID, shifted and semantic OOD sets

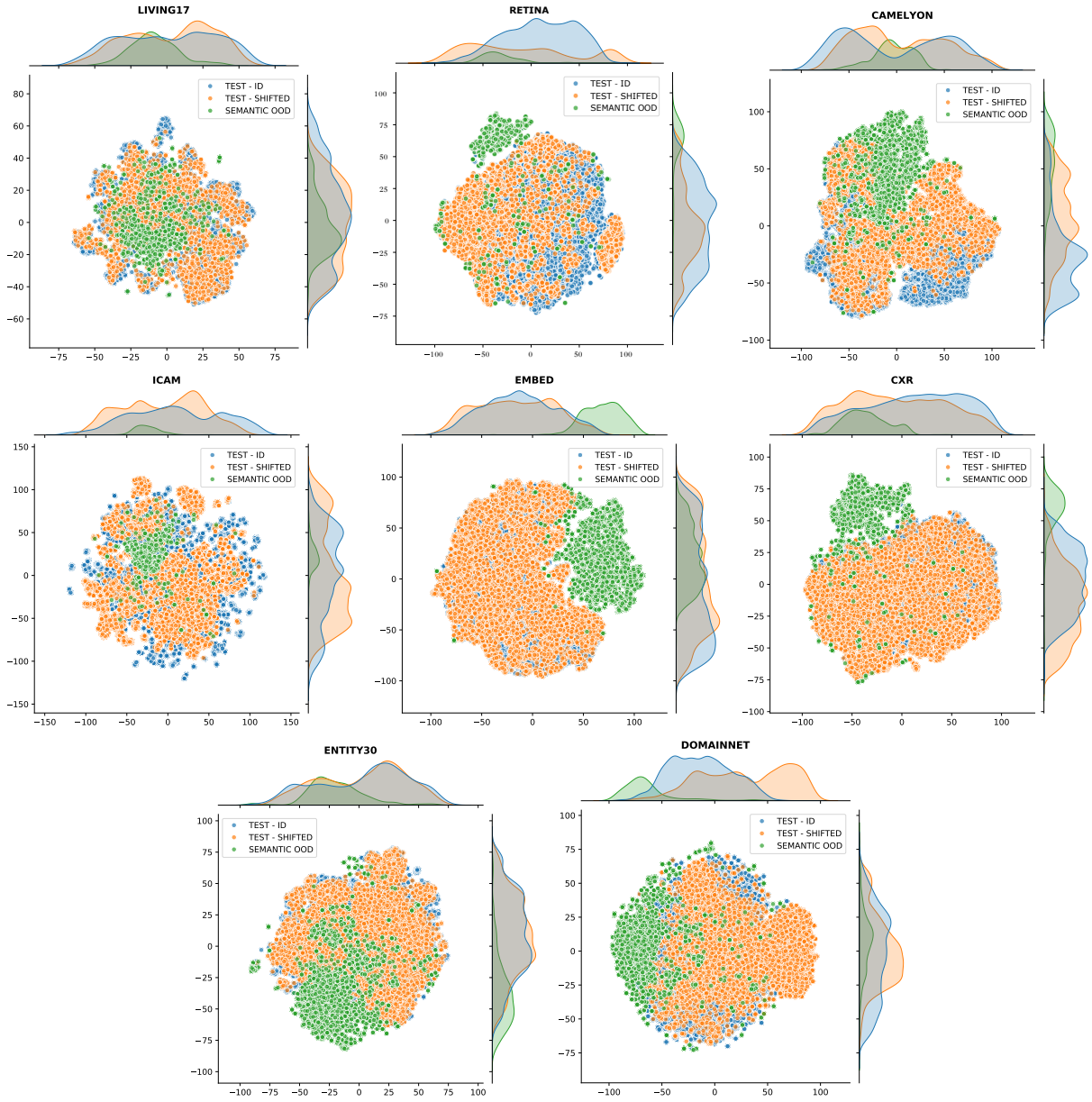

Figure A.3: **Embedding space analysis across datasets with TSNE** (Maaten & Hinton, 2008). For every dataset, we analyse the distribution of the ResNet-18 classifier embeddings from ID test samples, shifted test samples and semantic OOD Textures samples. The TSNE representation is computed based on the entire set (ID + shifted + semantic OOD samples). Note that if either test set contains more than 10,000 samples, we randomly sampled a subset of 10,000 samples.

A.6 Balanced Accuracy results

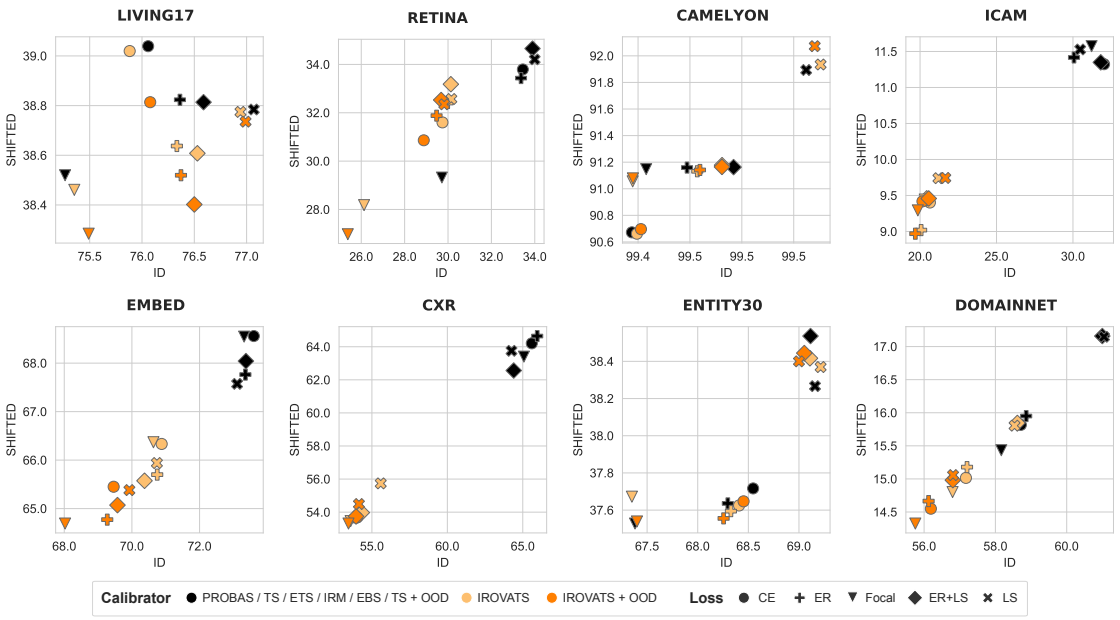

Figure A.4: **Balanced accuracy results (in %) on ID & shifted test sets, models trained from scratch**. Most post-hoc calibrators are accuracy-preserving, however IROVaTS is not and tends to decrease balanced accuracy across datasets. We do not observe any consistent performance differences across training losses.

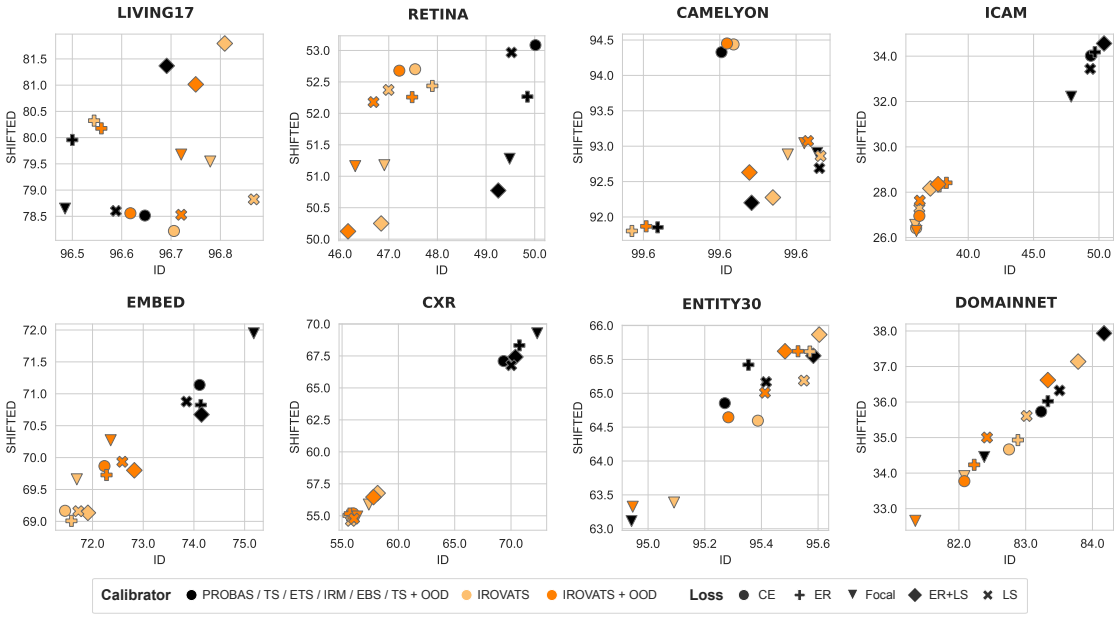

Figure A.5: **Balanced accuracy results (in %) on ID & shifted test sets, models finetuned from foundation models**. Most post-hoc calibrators are accuracy-preserving, however IROVaTS is not and tends to decrease balanced accuracy across datasets. We do not observe any consistent performance differences across training losses.

A.7 Statistical significance analysis

To determine the significance of the overall training loss + post-hoc calibrator 'treatment' effect across datasets and models, we use the Friedman (Friedman, 1937) and Nemenyi (Nemenyi, 1963) test. Technically, we run this test, separately for ID and OOD test sets. In our input data matrix, each row corresponds to one architecture-dataset combination for which we collect the average calibration error (across available test sets) for every treatment (loss + post-hoc calibrators). We find an overall significant effect with the Friedman test in both scenarios (ID and shifted). Hence, we follow by a Nemenyi post-hoc test to determine which treatment pairs have a significantly different treatment effect on the calibration results, results are presented in Fig. A.6.

We find that on shifted test sets, calibrators with semantic OOD exposure have a significantly different effect over those without OOD exposure, however there are no significant differences across calibrators once controlling for semantic OOD exposure (take-away 1). We also find that base probabilities from ER+LS models are not are not significantly different from any post-hoc calibration with OOD exposure (take-away 2). We find that, for nearly all post-hoc calibrators, after calibration there are no significant differences between different training losses. For ID sets, we find a significant effect of semantic OOD exposure as well, confirming the ID-OOD trade-off detailed in take-away 3.

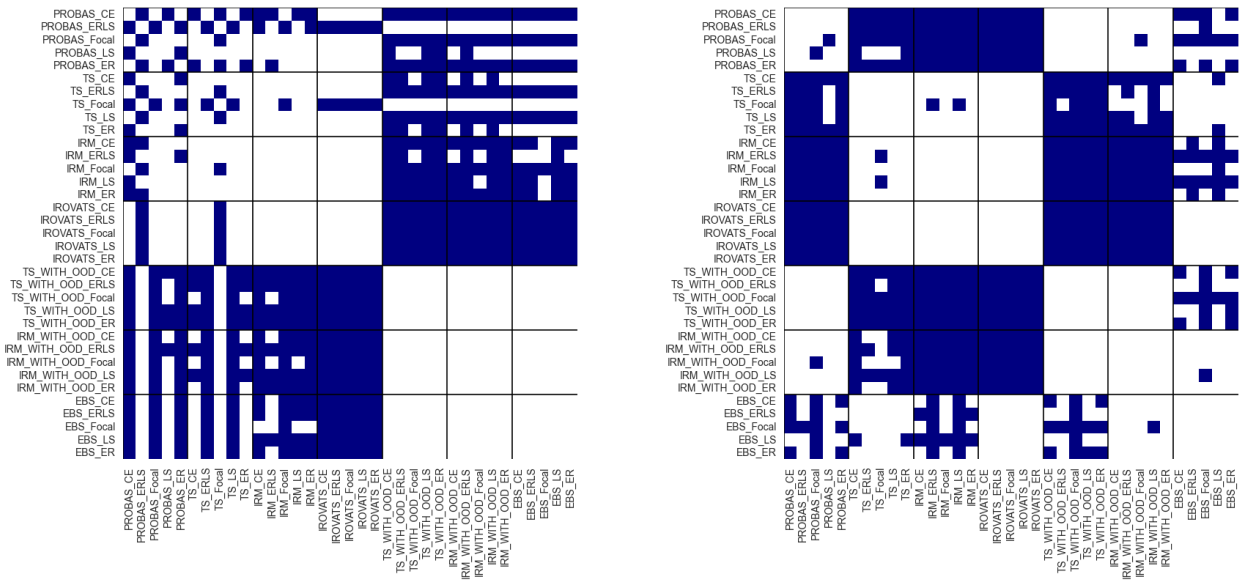

(a) Significant differences on shifted test sets

(b) Significant differences on ID test sets

Figure A.6: Full post-hoc comparison results of the Nemenyi test for ECE values on shifted and in-distribution test sets across all datasets and models (trained from scratch). The Nemenyi-post-hoc test identifies which specific treatments are significantly different from each other. Blue indicates a significant differences between the pairs of treatments in the x and y axes.

A.8 Detailed analysis of DAC effect

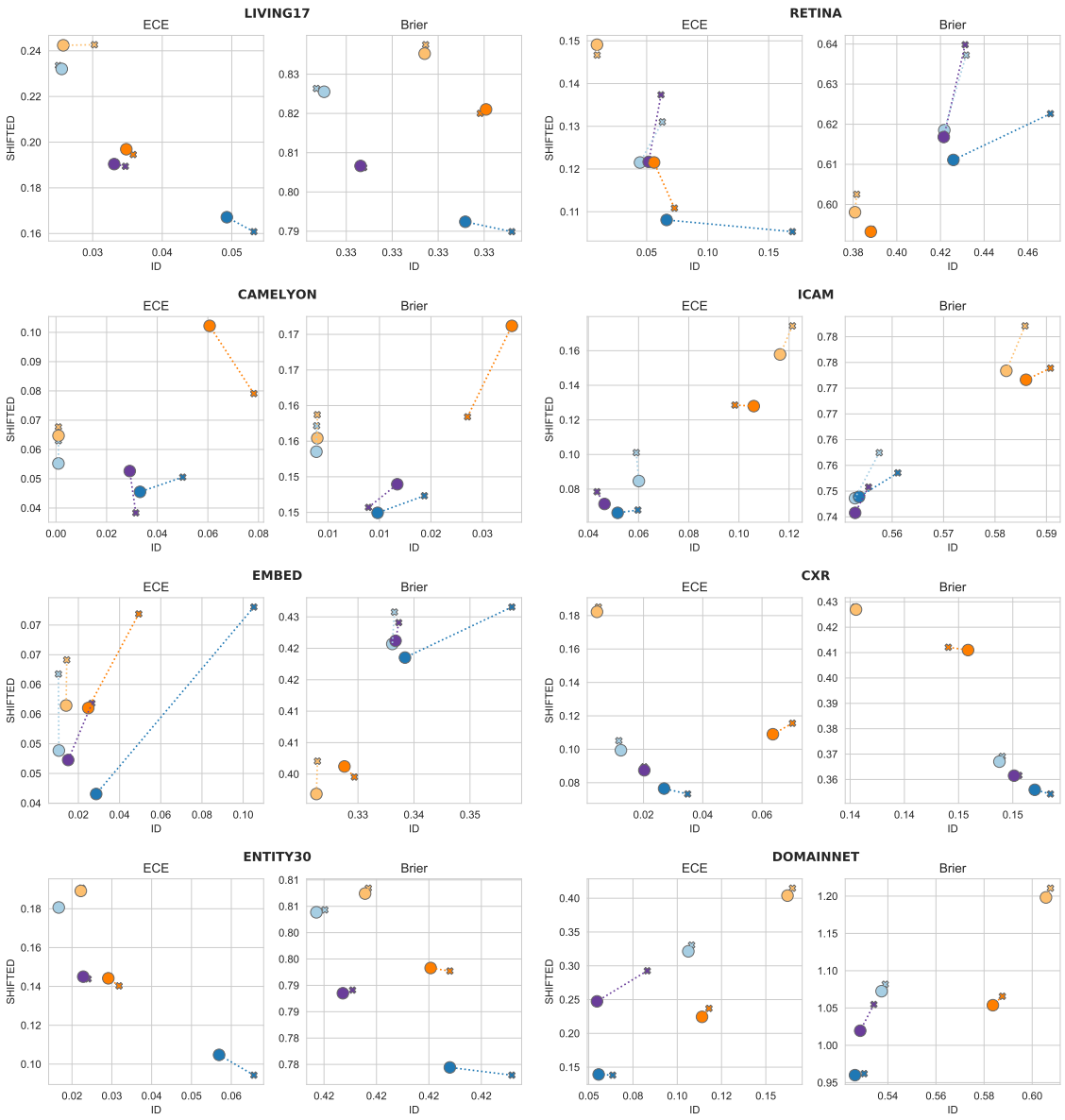

Figure A.7: **Detailed ablation results of DAC effect** in terms of average ECE and Brier score on ID and shifted test sets.

A.9 Ablation study: effect of model size on shifted calibration

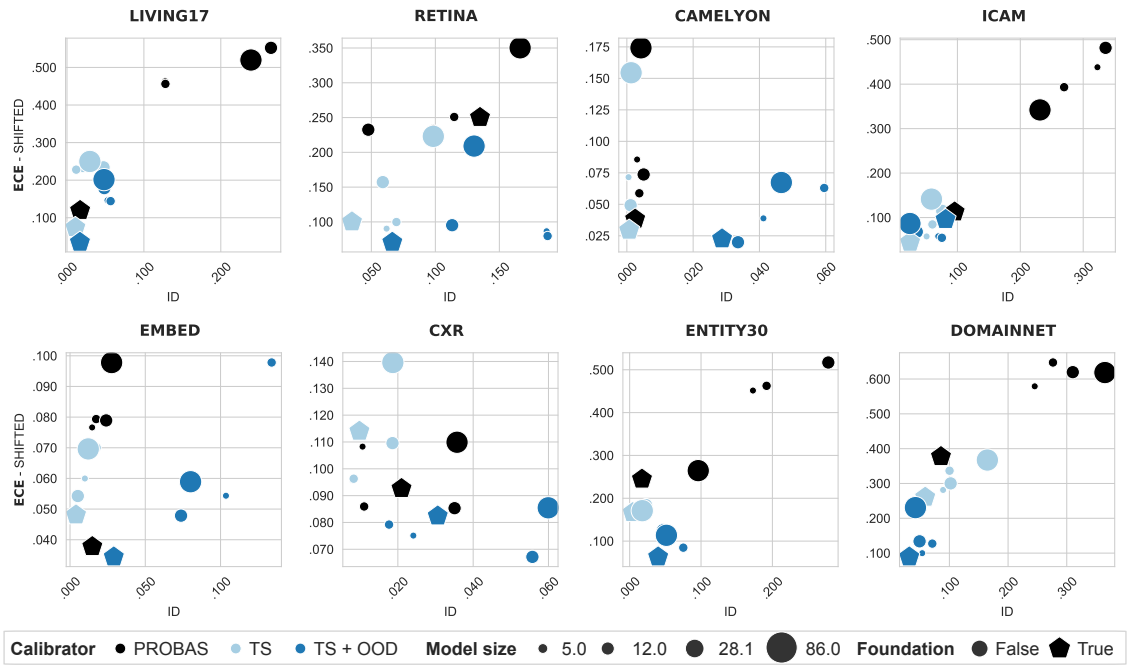

Figure A.8: **Ablation study: calibration results in function of model size**. We plot the ID-shifted ECE results by model size (for models trained from scratch) and compare with VIT-B-DINOv2 (i.e. finetuned from foundation model). We can see that calibration tends to degrade as model size increases. However, findings like benefit of semantic OOD exposure on shifted calibration and ID/shifted calibration trade-off hold irrespective of model size. Comparing ViT-B trained from scratch and from DINO, we see that calibration improvements are a consequence of pretraining, not of model size.

A.10 Additional figures for ensembles

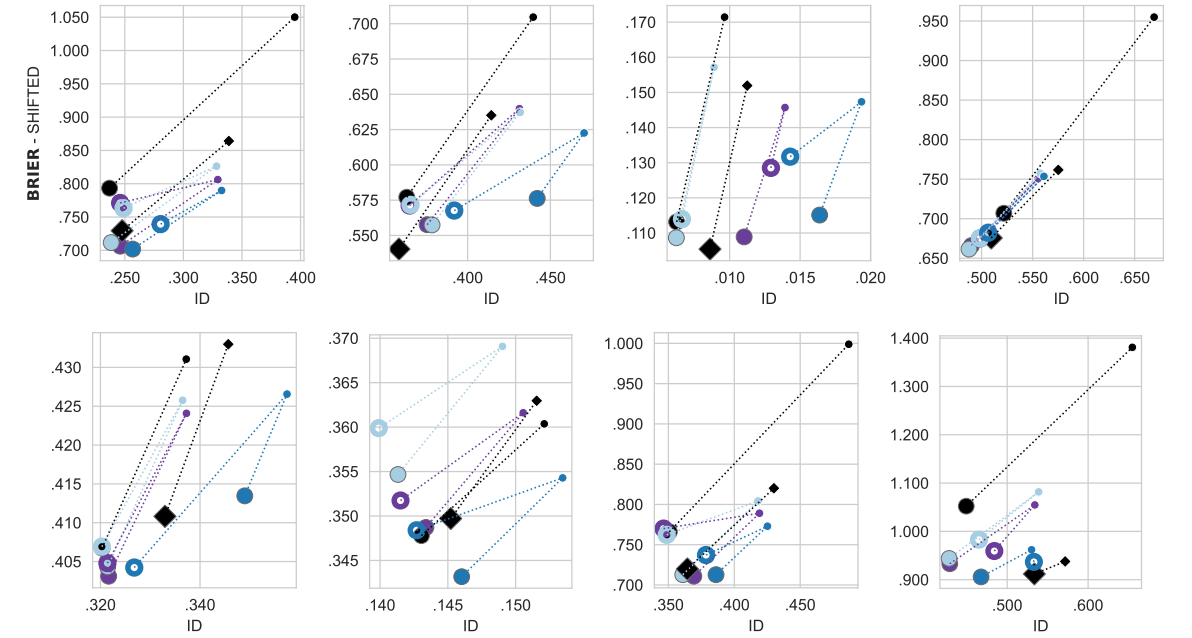

(a) Classifiers trained from scratch

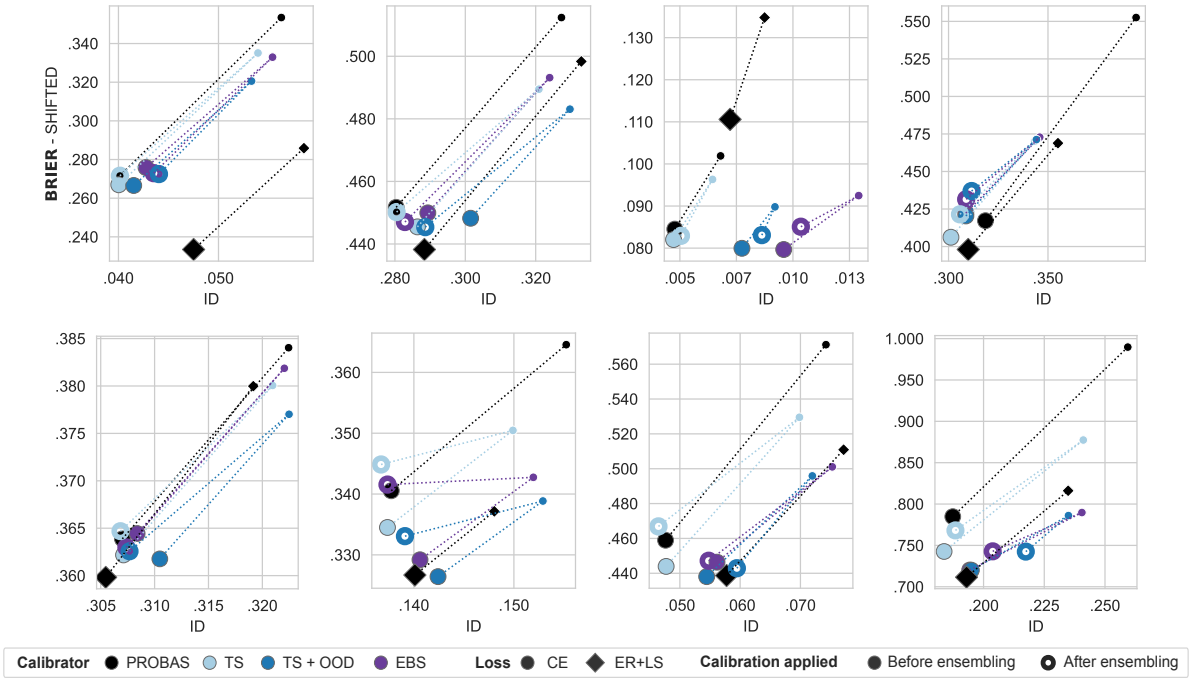

(b) Classifiers finetuned from foundation models

Figure A.9: **Brier score of model ensembles, in function of post-hoc calibration method** (3 member-ensembles). Large dots denote calibration results for model ensembles, small dots the average calibration of individual ensemble members for reference. We compare the effect of (i) applying post-hoc calibration to ensemble members (before ensembling), (ii) applying post-hoc calibration after ensembling predictions.

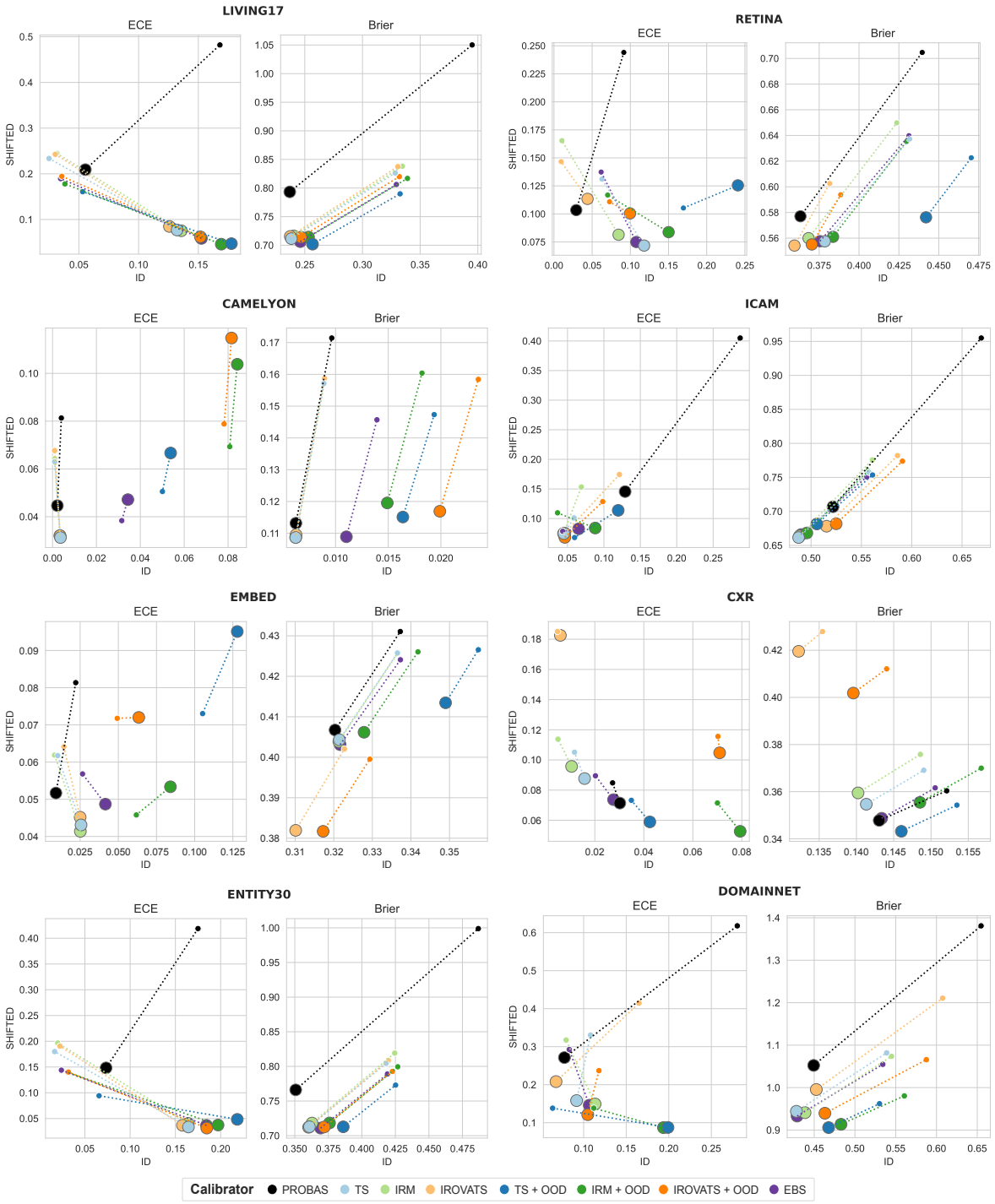

Figure A.10: **Ablation study of the effect of additional post-hoc calibrators of ensemble members** (prior to ensembling), for ensembles whose members were trained with CE (3 member-ensembles). Large dots denote calibration results for model ensembles, small dots denote the average calibration of individual ensemble members for reference.

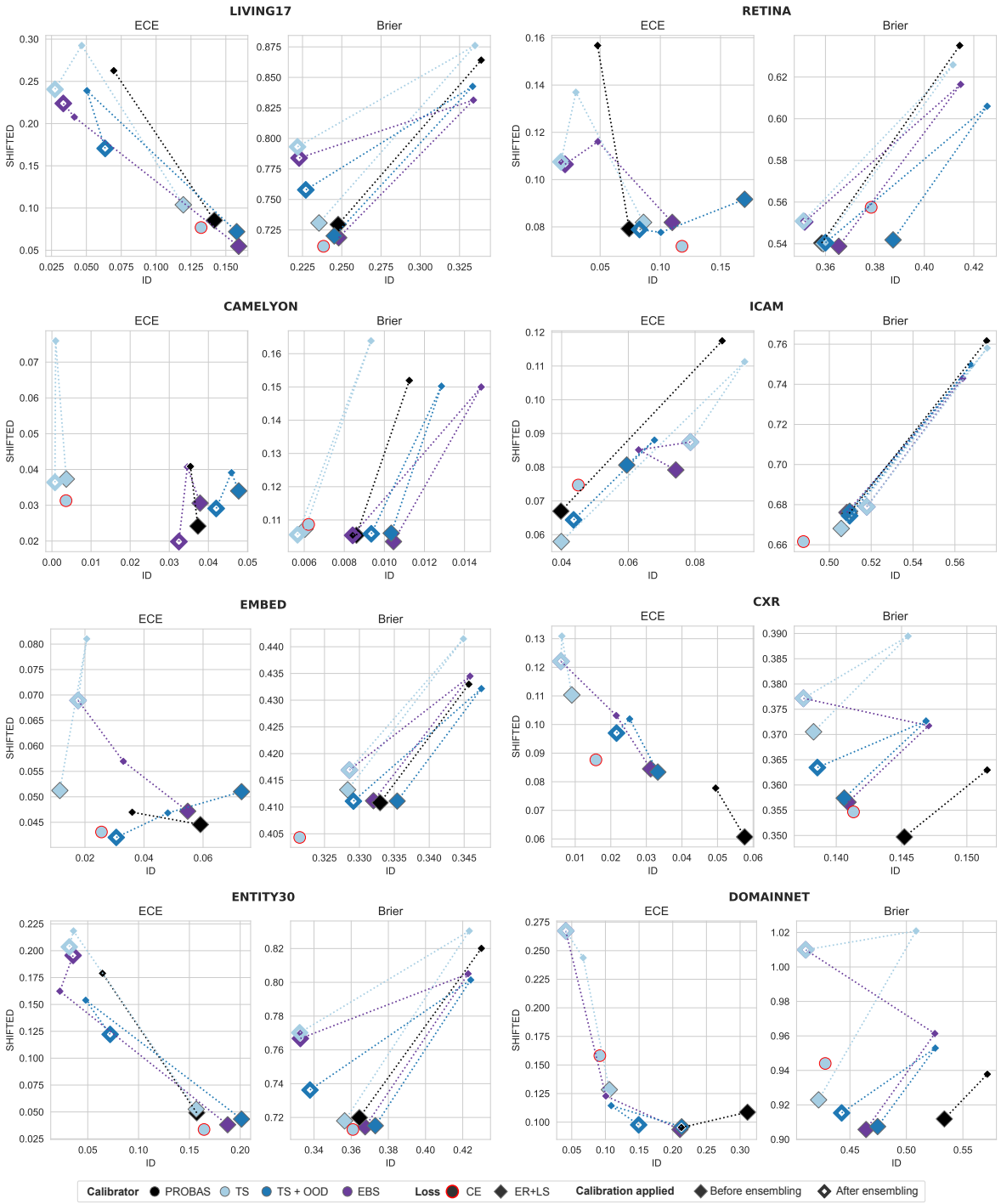

Figure A.11: **Calibration of model ensembles, in function of member calibration method, for ensembles whose members were trained with ERLS**. Large dots denote calibration results for model ensembles, small dots denote the average calibration of individual ensemble members for reference. We compare the effect of: (i) applying post-hoc calibration to ensemble members (prior to ensembling); (ii) applying post-hoc calibration after ensembling model predictions. We report calibration results for models trained with CE and with TS calibration post-ensembling as a baseline.

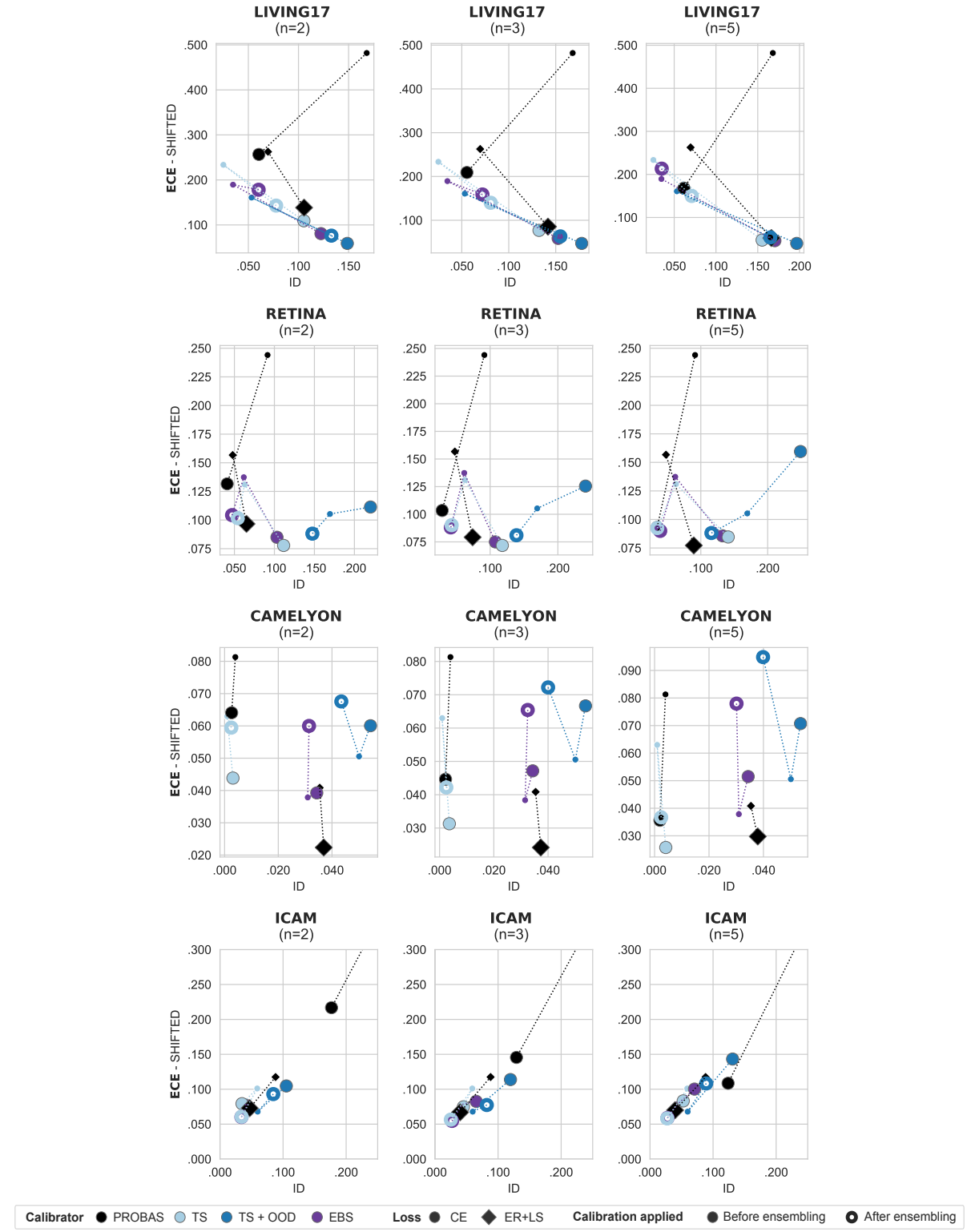

Figure A.12: **Calibration of model ensembles, in function of ensemble size and member calibration method, measured by ECE (1/2)**. Large dots denote calibration results for model ensembles, small dots denote the average calibration of individual ensemble members for reference. We compare the effect of: (i) applying post-hoc calibration to ensemble members (prior to ensembling); (ii) applying post-hoc calibration after ensembling model predictions. We report calibration results for models trained with CE and with TS calibration post-ensembling as a baseline.

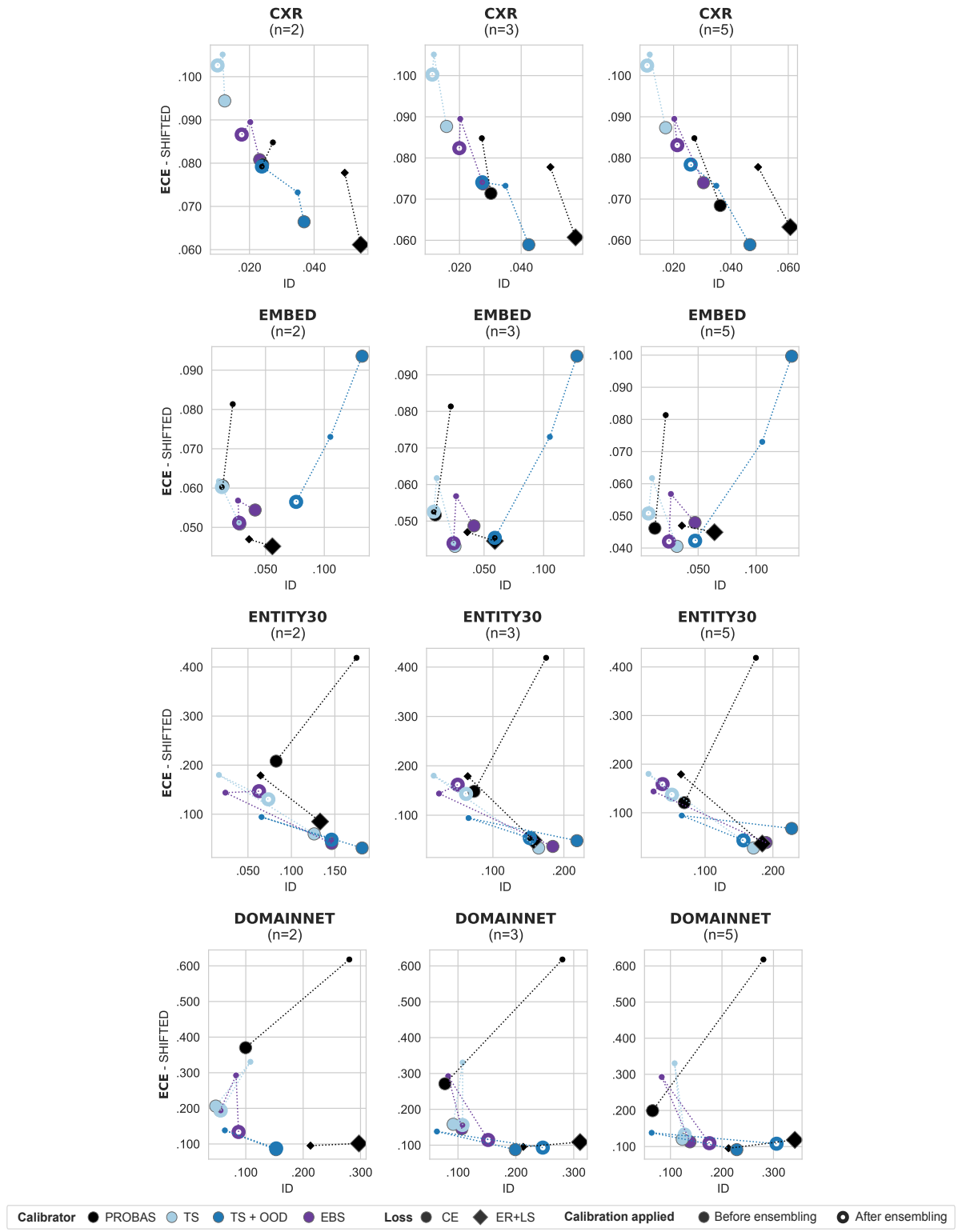

Figure A.13: **Calibration of model ensembles, in function of ensemble size and member calibration method, measured by ECE (2/2)**. Large dots denote calibration results for model ensembles, small dots denote the average calibration of individual ensemble members for reference. We compare the effect of: (i) applying post-hoc calibration to ensemble members (prior to ensembling); (ii) applying post-hoc calibration after ensembling model predictions. We report calibration results for models trained with CE and with TS calibration post-ensembling as a baseline.

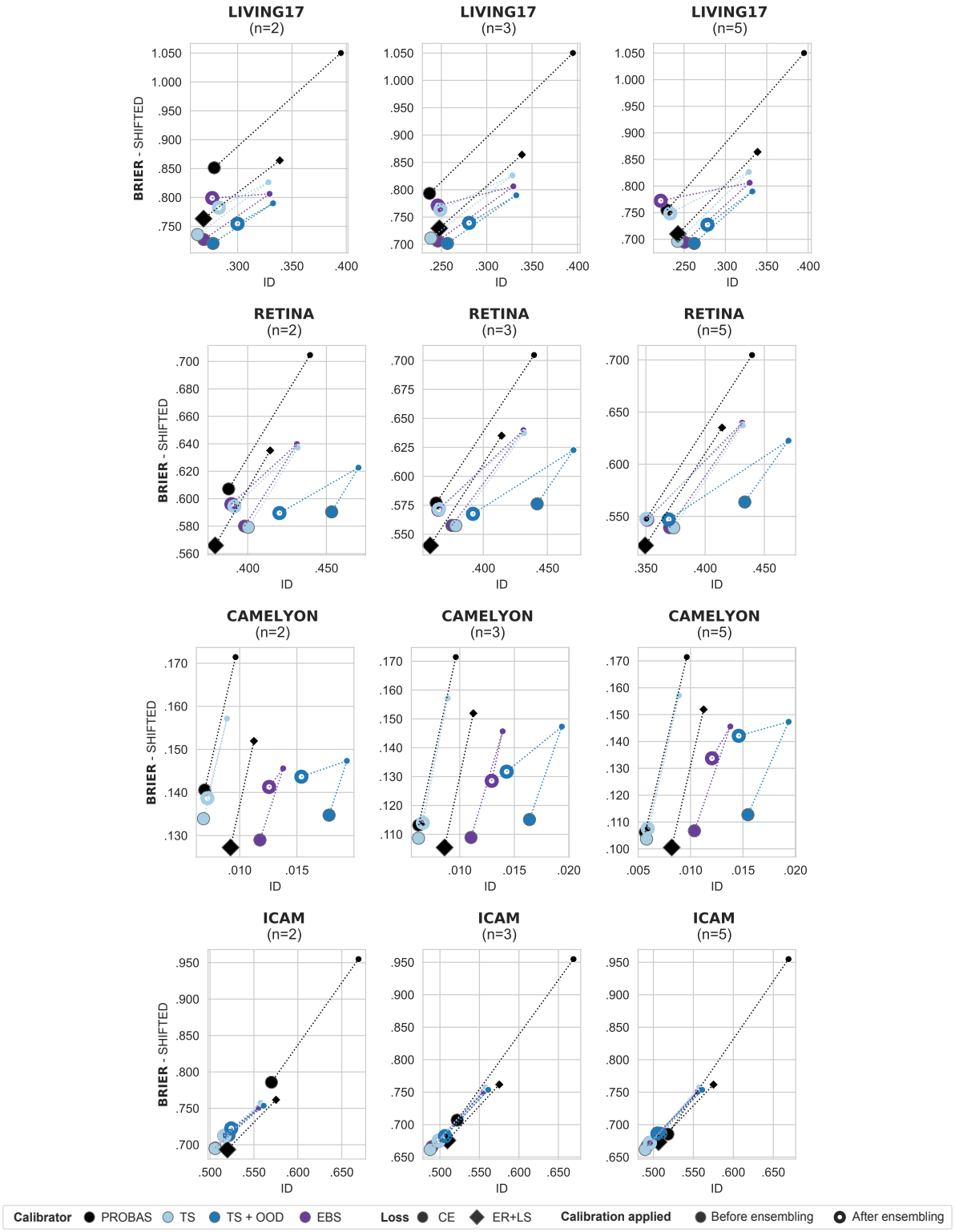

Figure A.14: **Calibration of model ensembles, in function of ensemble size and member calibration method, measured by Brier Score (1/2)**. Large dots denote calibration results for model ensembles, small dots denote the average calibration of individual ensemble members for reference. We compare the effect of: (i) applying post-hoc calibration to ensemble members (prior to ensembling); (ii) applying post-hoc calibration after ensembling model predictions. We report calibration results for models trained with CE and with TS calibration post-ensembling as a baseline.

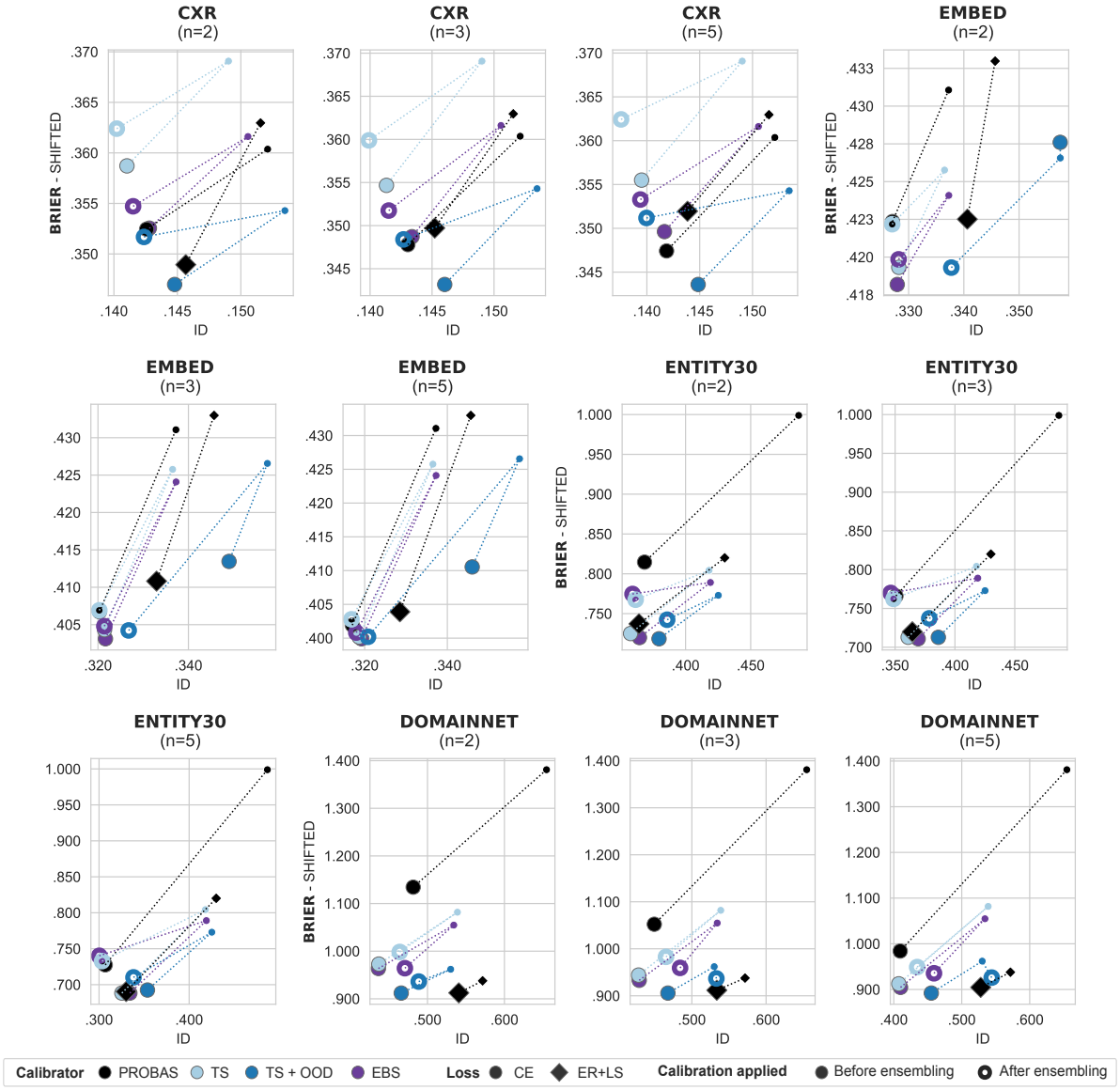

Figure A.15: **Calibration of model ensembles, in function of ensemble size and member calibration method, measured by Brier Score (2/2)**. Large dots denote calibration results for model ensembles, small dots denote the average calibration of individual ensemble members for reference. We compare the effect of: (i) applying post-hoc calibration to ensemble members (prior to ensembling); (ii) applying post-hoc calibration after ensembling model predictions. We report calibration results for models trained with CE and with TS calibration post-ensembling as a baseline.